

**Tubulobulbar Complexes Contribute to Basal Junction Remodeling in the Rat  
Seminiferous Epithelium**

by

Min Du

B.Sc., The University of British Columbia, 2009

A THESIS SUBMITTED IN PARTIAL FULFILLMENT OF THE REQUIREMENTS FOR

THE DEGREE OF

MASTER OF SCIENCE

in

The Faculty of Graduate Studies

(Cell and Developmental Biology)

THE UNIVERSITY OF BRITISH COLUMBIA

(Vancouver)

February 2013

© Min Du, 2013

## ABSTRACT

Tubulobulbar complexes are cytoskeleton-related membrane structures that develop at sites of intercellular attachment in the mammalian seminiferous epithelium. At apical junctions between Sertoli cells and spermatids the structures internalize adhesion junctions and are a component of the sperm release mechanism. Here I explore the possibility that tubulobulbar complexes that form at the ‘blood-testis barrier’ are sub-cellular machines that internalize basal junction complexes. Electron microscopy reveals that morphologically identifiable tight and gap junctions are present in basal tubulobulbar complexes in rats. In addition, immunological probes for claudin-11 (CLDN11), connexin-43 (GJA1), and nectin-2 (PVRL2) react with linear structures at the light level that I interpret as tubulobulbar complexes, and probes for early endosome antigen 1 (EEA1) and Rab5 (RAB5A) react in similar locations. Significantly, fluorescence staining patterns for actin and claudin-11 indicate that the amount of junction present is dramatically reduced over the time period that tubulobulbar complexes are known to be most prevalent during spermatogenesis. I also demonstrate, using electron microscopy and fluorescence microscopy, that tubulobulbar complexes develop at basal junctions in primary cultures of Sertoli cells. These structures not only morphologically resemble their *in vivo* counterparts, but they also contain junction proteins. I use this culture system together with transfection techniques to show that junction proteins from one transfected cell project into and are likely internalized by adjacent non-transfected cells as predicted by the junction internalization hypothesis. On the basis of my findings I present a new model for basal junction remodeling as it relates to spermatocyte translocation in the seminiferous epithelium.

## PREFACE

The majority of data and content in Chapters 1-5 of this thesis has been submitted for publication to the scientific journal 'Biology of Reproduction' under the title 'A Novel Subcellular Machine Contributes to Basal Junction Remodeling in the Seminiferous Epithelium', with contributions of all authors and collaborators described as follows. Min Du, myself, was responsible for the establishment and maintenance of primary Sertoli cell cultures (the basis upon which all *in vitro* data and images were acquired), preparation of various stock and working solutions (examples include enzyme solutions, stock components of specialized culture media, specialized culture media and DNA transfection mixes), immunofluorescence preparation of both *in vitro* and *in vivo* (tissue sections and tissue fragments) samples, acquisition of digital images using conventional and confocal microscopes, generation of DNA plasmids that incorporated a claudin-11-GFP fusion construct (with significant aid from a co-author as indicated below) and general preparation of labstuff (such as aliquoting reagent stock solutions, purchasing, preparing experimental tools and equipment). J'Nelle Young performed statistical analysis of the data that compare the amounts of basal junction material at Stages V and VII of the rat seminiferous epithelium, and offered numerous advice on immunofluorescence preparation and image acquisition. Marc De Asis was physically involved in several cell culture experiments by helping to complete certain steps in the cell isolation process. Jane Cipollone trained me on the crucial basic cell culture techniques. Dr. Calvin Roskelley provided the essential equipment with which to perform the cell culture experiments. Dr. Yoshimi Takai provided an anti-nectin-2 primary antibody that was not commercially available. Peter K. Nicholls, whose supervisor is Dr. Peter G. Stanton, donated the claudin-11 cDNA with which the GFP-tagged fusion construct was made. Dr. Wanyin Deng trained me on the techniques of DNA plasmid construction and was extensively involved in the actual making of the GFP-tagged claudin-11 fusion construct. Dr.

Brett Finlay is the head of the research group that Dr. Deng belongs to and provided the equipment and reagents with which to construct DNA plasmids. Dr. Wayne Vogl was my Master's degree supervisor and has given tremendous amounts of help and training to my thesis work. Dr. Vogl was physically involved in the tissue preparation and immunofluorescence image acquisition of both *in vitro* and *in vivo* experiments, and has provided excellent electron micrographs for this thesis.

All fluorescence images presented in this thesis were acquired, processed and composed into figures by me with the exceptions of Fig. 5 and Fig. 6. Fig. 16 and Figure 17 were also composed by me. Suggestions on image arrangement in figures were provided by Dr. Vogl. Adjustments on image placement within a figure, positioning of arrowheads and image labels were made by Dr. Vogl. All electron micrographs and relevant figures were acquired and composed by Dr. Vogl. For *in vitro* experiments, rat testes were surgically removed from animals under deep anesthesia by Dr. Vogl, and subsequent cell isolation, seeding, maintenance and fluorescence preparation were performed by myself. For *in vivo* experiments, testes removal and fixation, as well as tissue sections and tissue fragmentation were performed by Dr. Vogl, with subsequent immunofluorescence preparations performed by myself. The construction of GFP-tagged claudin-11 fusion construct was led by Dr. Wanyin Deng and I was involved in completing the different steps involved.

This thesis is based on the manuscript written by me and Dr. Vogl that has been published by Biology of Reproduction online ahead of print on January 9, 2013. To complete the thesis, I have added to the manuscript further content such as new figures (Fig. 14 to 17), edits to figures (Fig. 1, 4, 5, 6, 7 and 13), relevant figure legends, the entirety of Chapter 6, new content in Chapters 3-4 regarding the added data and figures, additional information in Chapters 1-2, the Preface, the Table of Contents, the List of Figures, and various other content to comply with the UBC Faculty of Graduate Studies approved thesis structure and flow.

The use of animals in this study has been approved by the Animal Care Committee of the University of British Columbia. Approved animal care protocols are A12-0108 and A11-0172.

## TABLE OF CONTENTS

ABSTRACT .....	ii
PREFACE.....	iii
TABLE OF CONTENTS .....	vi
LIST OF FIGURES .....	viii
ACKNOWLEDGEMENTS.....	ix
DEDICATION .....	x
CHAPTER 1: INTRODUCTION .....	1
Background.....	1
Spermatogenesis .....	1
Stages of the cycle of the seminiferous epithelium .....	3
Basal junction turnover in the seminiferous epithelium .....	5
Basal Tubulobulbar Complexes.....	5
Primary Sertoli cell cultures.....	6
Hypothesis.....	7
Summary of results.....	8
CHAPTER 2: MATERIALS AND METHODS .....	10
Animals.....	10
Primary Sertoli cell culture .....	10
Composition of serum-free defined medium (SFDM).....	13
Transfection of cultures with plasmids.....	13
Construction of claudin-11-GFP plasmids .....	14
Immunofluorescence of Sertoli cell cultures.....	15
Immunofluorescence of tissue sections and tissue fragments.....	16
Antibodies and stains .....	17
Estimation of Sertoli cell culture purity by cell counting .....	19
Electron Microscopy .....	20
3D analysis of confocal Z-stacks.....	20

Analysis of junction staining .....	21
CHAPTER 3: RESULTS .....	22
Basal tubulobulbar complexes form within junction ‘pockets’ .....	22
Basal tubulobulbar complexes contain morphologically identifiable intercellular junctions....	22
Basal tubulobulbar complexes contain claudin-11, connexin-43 and nectin-2.....	23
The endocytic markers EEA1 (early endosome antigen 1) and Rab5 associate with basal tubulobulbar complexes .....	23
Basal junctions are less apparent after the peak appearance of tubulobulbar complexes.....	24
Basal tubulobulbar complexes form in primary cultures of rat Sertoli cells .....	25
Tubulobulbar complexes <i>in vitro</i> contain morphologically identifiable junctions .....	27
Tubulobulbar complexes in primary Sertoli cell cultures contain junction proteins.....	27
Junction proteins from one Sertoli cell are internalized by neighboring Sertoli cells .....	28
Sertoli cell cultures are approximately 85% pure.....	29
CHAPTER 4: DISCUSSION .....	31
The role of basal tubulobulbar complexes in junction internalization .....	31
Tubulobulbar complexes in the <i>in vitro</i> system .....	33
The role of basal tubulobulbar complexes in spermatocyte translocation.....	34
Overview of conclusions .....	36
CHAPTER 5: FIGURES .....	37
CHAPTER 6: CONCLUDING CHAPTER.....	60
Relevance and contributions to the field.....	60
Overview of results and conclusions.....	62
Limitations .....	62
Future directions.....	63
A potential contraceptive target.....	66
REFERENCES.....	68

## LIST OF FIGURES

FIG. 1. Schematic diagram of a tubulobulbar complex and seminiferous epithelium. ....	37
FIG. 2. Electron micrographs of basal junction complexes between Sertoli cells and associated tubulobulbar complexes. ....	38
FIG. 3. Confocal images of putative basal tubulobulbar complexes in cryo-sections of adult rat seminiferous epithelia approximately at Stage V of spermatogenesis. ....	41
FIG. 4. Confocal images of basal junction regions in adult rat seminiferous epithelia immunoprobed for endocytic markers EEA1 (early endosome antigen 1) and Rab5. ....	42
FIG. 5. Conventional immunofluorescence images of 5 µm thick cryo-sections from perfusion fixed rat testis labeled for actin. ....	43
FIG. 6. Conventional immunofluorescence images of 5 µm thick cryo-sections from perfusion fixed rat testis labeled for claudin-11. ....	44
FIG. 7. Primary cultures of Sertoli cells grown on Matrigel™ in transwells are morphologically differentiated and form basal junction complexes. ....	47
FIG. 8. Ultrastructural evidence for the formation of tubulobulbar complexes at intercellular junctions in primary cultures of Sertoli cells. ....	48
FIG. 9. Electron microscopic images of tubulobulbar-like structures in primary cultures of Sertoli cells. ....	51
FIG. 10. Electron micrographs of tubulobulbar complexes in primary cultures of Sertoli cells showing the presence of ‘membrane kisses’ (arrowheads) indicative of tight junctions and similar to those observed at similar locations <i>in vivo</i> . ....	51
FIG. 11. Confocal (single plane) images of putative tubulobulbar complexes between cultured Sertoli cells. ....	52
FIG. 12. Confocal images of cultured Sertoli cells labeled for AP2. ....	53
FIG. 13. Confocal images showing cultured Sertoli cells transfected with DNA plasmids encoding GFP-tagged junction proteins extend rod-like structures into adjacent non-transfected Sertoli cells. ....	54
FIG. 14. Confocal images of cultured Sertoli cells showing possible tubulobulbar complexes capped at their ends by the endocytic markers EEA1 or Rab5. ....	55
FIG. 15. Confocal images of cultured Sertoli cells showing controls for <i>in vitro</i> transfection applications. ....	56
FIG. 16. Restriction digests of the pCR2.1-TOPO, pEGFP-N1 and pEGFP-C1 vectors used in the making of the claudin-11-GFP fusion construct. ....	57
FIG. 17. Schematic representation of major steps during basal tubulobulbar complex-mediated junction internalization. ....	58

## ACKNOWLEDGEMENTS

I wish to express sincere gratitude to faculty and staff members of the Faculty of Cellular and Physiological Sciences at the University of British Columbia, whose devotion to teaching and passion for science have inspired me to complete my thesis. I thank Dr. Roskelley and members of his research team who generously accommodated me and allowed me to use their equipment. I thank my committee members, Dr. Roskelley and Dr. O'Connor, for taking time from their busy schedules to check my degree progress during committee meetings and to offer helpful advice on how to strengthen my work. I thank Pascal St-Pierre for providing detailed and helpful guidance to the three dimensional reconstruction software. I also thank the staff members at the Centre for Disease Modeling for the care that they provided to our experimental animals.

I thank all members of the Vogl Lab for being a fantastic team to work with, especially Dr. Wayne Vogl. Dr. Vogl is an extraordinary supervisor whose extensive involvement in bench work, upbeat personality and strong scientific expertise have greatly inspired me. Dr. Vogl also was amazingly patient and helpful with me during the entire course of my thesis work. I would like to express sincere gratitude to Marc De Asis and Alex Chan for their support and for physically helping me to complete certain steps in my experiments on numerous occasions. I thank J'Nelle Young for the scientific advices that she had given me, for teaching me some of the basics of laboratory conduct and for helping to perform the statistical analysis that is included in this thesis. I also thank NSERC for providing the research grant that funds my work.

I would like to express a heartfelt appreciation to my family and friends for their support during my graduate studies. Without them I would not be able to complete this work.

## **DEDICATION**

*To my parents, whose unconditional love and support made this work possible.*

## **CHAPTER 1: INTRODUCTION**

Intercellular junction turnover is a fundamental property of cells. It not only is important during morphogenesis, but also occurs during epithelial renewal, the movement of cells between compartments, and tumor progression. A currently accepted model for junction disassembly is one in which integral membrane junction molecules in adjacent cells detach from each other and are internalized into each of the parent cells by conventional mechanisms of endocytosis [1-4] or macropinocytosis [5-7]. An exception to this occurs with gap junctions that are internalized as intact junctions in large double membrane vesicles into one or the other of the attached cells [8-10] in a clathrin mediated fashion [11]. An entirely different mechanism of junction internalization may occur at basal junction complexes between Sertoli cells in the seminiferous epithelium of the mammalian testis and is the focus of this thesis.

### **Background**

#### **Spermatogenesis**

The mammalian testis houses a variety of anatomical features, one of which is the collection of small coiled tube-like structures termed seminiferous tubules, or ‘sperm-producing’ small tubes. The lumen of each tubule is lined by a seminiferous epithelium that is formed by columnar epithelial cells called Sertoli cells as well as developing germ cells that migrate between the Sertoli cells toward the lumen of the seminiferous tubule. The developing germ cells undergo spermatogenesis, the complicated multi-step biological process by which spermatogonia develop into primary and secondary spermatocytes and eventually into mature spermatozoa.

Similar to other types of epithelial cells, Sertoli cells connect with each other via junction complexes. In the seminiferous epithelium, these junction complexes are located near the

basement membrane and are composed in part by adhesion (ectoplasmic specializations [12]), tight and gap junctions. Tight junctions form the blood-testis barrier that separates the epithelium into two compartments: a basal compartment where early spermatogenic cells are located and an adluminal one that contains ‘late’ spermatocytes and spermatids [13]. During meiosis, spermatocytes are translocated from basal into adluminal compartments. In the rat seminiferous epithelium, different types of intercellular junctions employ different integral membrane proteins to facilitate linkage between neighboring Sertoli cells. Among others, claudins and occludins are present at tight junctions, one of which is claudin-11 [14]. Nectin-2 is an integral membrane protein that participates in homotypic intercellular junctions at basal ectoplasmic specializations [15], while connexin-43 is a component of the gap junctions between Sertoli cells [14].

Claudin-11, also known as the oligodendrocyte-specific protein (OSP), is an integral membrane protein with a molecular mass of approximately 22 kD and is expressed by oligodendrocytes in the brain and by Sertoli cells in the testis [14, 16]. Claudins have been suggested to bind with ZO-1 which bridges the integral membrane proteins with the cytoskeleton [14]. In the testis, claudin-11 is a component of the tight junctions that form the blood-testis barrier [13, 16].

Nectin-2 belongs to an immunoglobulin-like family of adhesion junction proteins and has been shown to form a complex with the adaptor afadin which binds to filamentous actin [14, 17]. At apical ectoplasmic specializations, nectin-2 on the plasma membrane of a Sertoli cell connects heterotypically with nectin-3 on the plasma membrane of a spermatid [17]. At basal ectoplasmic specializations, nectin-2 on the plasma membrane of a Sertoli cell connects homotypically with another nectin-2 molecule on a neighboring Sertoli cell [15].

A major component of gap junctions are connexins, which are integral membrane proteins that complex with each other to form hexameric hemi-channels termed connexons on

the plasma membrane [18]. A connexon on the plasma membrane of one cell interacts with and binds to another connexon on a neighboring cell, thus completing a channel that permits the exchange of various substances between the two cells [18-20]. Different types of connexins are named based on the molecular mass predicted from their cDNA sequences [18, 20]. In the testis, connexin-43, which has a molecular mass of 43.0 kDa [18], is the major type of connexin that can be found in Sertoli cells at basal junction regions [19, 20].

### **Stages of the cycle of the seminiferous epithelium**

Spermatogenesis is a complex multi-step process. In the rat, successive generations of spermatogenic cells continually undergo spermatogenesis at each location within the seminiferous tubule. That is, before one generation of spermatogenic cells completes spermatogenesis, the next generation will arise from spermatogonia and begin the same process at the location in the seminiferous epithelium where the prior generation first arose. Along each seminiferous tubule, segments of the epithelium are arranged in order so that one segment is slightly ahead of the development of the segment behind. As the generations of spermatogenic cells progress through spermatogenesis, a series of distinctive cellular associations occurs and each cellular association is characteristic of the step(s) of spermatogenesis that the cells are in at a give point in time (or steps of spermiogenesis, which were the basis upon which the stages were first defined). At any cross-section of the seminiferous tubule in rat, a unique cellular association can be seen and defines a certain stage of the cycle. Depending on the particular stage, different numbers of generations of spermatogenic cells may be seen in a cross-section of the seminiferous epithelium. Overall, fourteen stages of the seminiferous epithelium can be identified in the rat, each designated by a corresponding roman numeral. For the purpose of this thesis, only Stages V and VII will be briefly described. Descriptions of all stages of the cycle of

the seminiferous epithelium in the rat and of methods to identify the stages can be found in the reports by Leblond and Clermont [21] and Clermont and Perey [22]. The completion time for one cycle is approximately twelve days [23, 24].

At Stage V of the cycle of the seminiferous epithelium, spermatocytes of a younger generation continue to grow while maturing spermatids of an older generation are entrenched deep within the seminiferous epithelium. Maturing spermatids are grouped in bundles and their nuclei are situated in proximity to the basement membrane. This positioning of bundles of spermatid nuclei close to the basement membrane can be used to identify Stage V of the cycle of the seminiferous epithelium in fluorescence or phase images.

At Stage VII of the cycle of the seminiferous epithelium, a newly-formed generation of spermatocytes is present along the basement membrane and an older generation of spermatocytes is at the pachytene stage of meiosis. Spermatids of an even older generation are situated apically in the seminiferous epithelium and line the lumen of the seminiferous tubule. Each maturing spermatid at Stage VII displays a curved nucleus. A lobule of Sertoli cell cytoplasm is present opposite to the concave surface of the curved nucleus. The presence of curved nuclei of maturing spermatids and their associated lobules of Sertoli cell cytoplasm that line the lumen of the seminiferous tubule can be used to estimate Stage VII of the cycle of the seminiferous epithelium in fluorescence or phase images.

It also should be noted that the newly-formed generation of spermatocytes begin their translocation from the basal compartment into the adluminal compartment approximately in Stage VIII of the cycle of the seminiferous epithelium [25].

## **Basal junction turnover in the seminiferous epithelium**

In the seminiferous epithelium, the translocation of spermatocytes from basal to adluminal compartments through massive and basally situated intercellular junctions between Sertoli cells is fundamental to male fertility. The adluminal compartment is where spermatocytes complete meiosis and the resulting haploid spermatids ultimately differentiate into male gametes that are released from the epithelium as spermatozoa. During the translocation event, junctions disassemble above spermatocytes and simultaneously assemble below [25, 26], thereby maintaining the Sertoli cell permeability barrier and the integrity of the adluminal compartment of the epithelium. In addition, unique sub-cellular structures called tubulobulbar complexes form at basal junctions in the seminiferous epithelium and several different functions were proposed for them, some of which were described in a recent review [27]. The function that I favor is one where basal tubulobulbar complexes are thought to internalize basal junctions into one or the other of the attached Sertoli cells [28].

## **Basal Tubulobulbar Complexes**

Tubulobulbar complexes at basal junctions in the seminiferous epithelium consist of long tubular extensions from one Sertoli cell that project into corresponding invaginations of the neighboring Sertoli cell (Fig. 1)[28]. This double membrane core is cuffed by a network of actin filaments along its length, and at the tip of the complex is a coated-pit. The distal third of the double-membrane tube becomes swollen and the actin cuff is replaced by a cistern of endoplasmic reticulum. This bulbar region eventually buds off from the complex and is internalized by the Sertoli cell [29].

Since their first discovery over four decades ago, there have been few detailed studies on basal tubulobulbar complexes and the structures have generally been ignored in discussions of spermatocyte translocation. This is somewhat surprising because the complexes have long been speculated to be involved with basal junction turnover [15, 29, 30], and similar tubulobulbar complexes that form at apical sites of attachment between Sertoli cells and mature spermatids have been shown both to internalize adhesion junctions [31-33] and to be linked to the mechanism of sperm release [34-36]. In addition, there is a burst in basal tubulobulbar complex formation that precedes the translocation of spermatocytes from basal to adluminal compartments of the epithelium [29], an observation consistent with a role in junction remodeling associated with the translocation event.

The lack of studies on basal tubulobulbar complexes is likely due to a number of factors. First, the structures are notoriously difficult to distinguish from elements of the junction complex using conventional fluorescence microscopy. Second, unlike apical tubulobulbar complexes that are clustered in specific regions adjacent to spermatid heads, basal complexes do not cluster at any specific and predictable location at the belt-like junctions between neighboring Sertoli cells. Finally, basal complexes cannot be isolated in a similar fashion to apical complexes for visualization at high resolution. An additional problem for studying tubulobulbar complexes in general is that no model system has been developed for experimentally manipulating the structures *in vitro*.

### **Primary Sertoli cell cultures**

Up to now, scientists in the field have been using primary cultures of rat Sertoli cells as a tool in research for more than thirty-five years [37-48]. Earlier methods for establishing primary

Sertoli cell cultures involved isolating Sertoli cells from testicular tissue through serial enzymatic digestions and mechanical agitations, as well as seeding the isolated Sertoli cells onto the bottoms of culture flasks or dishes [37, 38]. Since then, the culture technique has been progressively improved as modifications were made that included the use of reconstituted basement membrane [49] as well as a dual-compartment culture chamber setup [39, 50-52]. With such improvements, cultured Sertoli cells are able to maintain morphological differentiation as reported by others [49, 50, 52].

A detailed description of the technique for establishing primary cultures of rat Sertoli cells can be found in the methods paper by Suarez-Quian and Onada [52]. This technique involves the use of reconstituted basement membrane (Matrigel<sup>TM</sup>) in a dual-compartment culture chamber setup. Sertoli cells from rats between 10 to 30 days of age should be used for primary cell cultures, as it is more difficult to isolate Sertoli cells from older and more mature rats due to increased amounts of germ cell contamination and of connective tissue [52]. When Sertoli cells from 20-day-old rats are used, the seeding density must be high because the mitotic activities of Sertoli cells are reduced after approximately two week post-birth [53, 54] and therefore will not divide sufficiently to reach confluency when seeded at low densities. A subsequent hypotonic treatment to the cultures can be performed to improve Sertoli cell purity in culture [40].

## **Hypothesis**

In this thesis, I hypothesize that basal tubulobulbar complexes are sub-cellular machines that internalize basal intercellular junction proteins into one or the other of the attached Sertoli cells in the mammalian seminiferous epithelium. To test this hypothesis, one of my aims is to

explore the possibility of using primary cultures of rat Sertoli cells as an *in vitro* tool for the study of basal tubulobulbar complexes. If the junction internalization hypothesis is true, then basal junction proteins should be present within basal tubulobulbar complexes, endocytic markers should associate with basal tubulobulbar complexes and junction proteins from one Sertoli cell should be internalized into an adjacent Sertoli cell by basal tubulobulbar complexes. These predictions will be examined in this thesis.

### **Summary of results**

Here, electron microscopy demonstrates that basal tubulobulbar complexes *in vivo* often occur in pockets or folds formed by intercellular junctions, and I confirm an earlier report [28] that tight and gap junctions are present within the complexes. I extend these results by using confocal microscopy of perfusion fixed sections of rat testes immuno-labeled for the major protein components (nectin-2 [17], claudin-11 [16, 55], and connexin-43 [56-58]) of adhesion, tight and gap junctions in the epithelium to show that junction proteins are indeed present in the structures. Significantly, I show that the early endocytic markers (EEA1 and Rab5) are situated in similar locations. In addition, there appears to be less basal junction present at Stage VII than at Stage V, an observation that correlates with the time during which basal tubulobulbar complexes are known to be most active during spermatogenesis. I demonstrate for the first time that tubulobulbar complexes develop in a primary Sertoli cell culture system. Furthermore, I use this *in vitro* model system together with immunofluorescence and transfection techniques to show that, like their *in vivo* counterparts, the structures contain junction proteins. The identity of tubulobulbar complexes in fluorescence data was determined by using filamentous actin or the clathrin related protein AP2 as markers. In addition, tight junctions ('membrane-kisses') are visible in the structures when evaluated by electron microscopy. I conclude that basal

tubulobulbar complexes internalize intercellular junctions between Sertoli cells and therefore may significantly contribute to junction remodeling at the blood-testis barrier and to the mechanism by which spermatocytes translocate from basal to adluminal compartments of the seminiferous epithelium.

## **CHAPTER 2: MATERIALS AND METHODS**

### **Animals**

All animals used in the study were Sprague Dawley rats obtained from Charles River (Sherbrooke, QC, Canada). They were housed and used in accordance with guidelines established by the Canadian Council on Animal Care and according to protocols approved by the Animal Care Committee of the University of British Columbia. Twenty-day-old pups were obtained from a small breeding colony maintained in our animal care facility.

### **Primary Sertoli cell culture**

Primary Sertoli cell cultures were prepared based on established protocols [49, 51, 52]. In my hands, the cultures were approximately 85% Sertoli cells, with contaminants being germ cells and myoid cells.

One day prior to Sertoli cell isolation, a cell culture plate was prepared by adding Falcon™ cell culture inserts (bottom filter membrane contains 1 µm-sized pores) (BD Biosciences, Mississauga, ON, Canada) into wells of a Falcon™ 24-well Multiwell Plate (BD Biosciences, Mississauga, ON, Canada). Matrigel™ (BD Biosciences, Mississauga, ON, Canada) was diluted 1:5 with DMEM/F12 containing L-Glutamine and antibiotics, and 50 µl of diluted Matrigel™ was used to coat each filter membrane. Diluted Matrigel™ was allowed to polymerize at 37°C overnight.

To isolate Sertoli cells from fresh rat testicular tissue, twenty-day-old Sprague-Dawley rat pups were put under deep anesthesia with isoflurane, the animals were euthanized by decapitation, and then their testes removed. Testes were decapsulated, minced into a fine slurry

and transferred to a sterile dissociation flask (Fisher Scientific, Ottawa, ON, Canada) containing 20 ml of the first enzyme solution [DMEM/F12 containing 1.5 mg/ml trypsin (STEMCELL Technologies, Vancouver, BC, Canada), 40 µg/ml crude Deoxyribonuclease I (Sigma-Aldrich, Oakville, ON, Canada), 250 ng/ml fungizone (HyClone, Logan, UT, USA), 100 U/ml penicillin (STEMCELL Technologies, Vancouver, BC, Canada) and 0.1 mg/ml streptomycin (STEMCELL Technologies, Vancouver, BC, Canada), non-sterile components were sterilized with 0.20 µm pore size syringe filters (Corning Incorporated, Corning, NY, USA) and 10 ml syringes (BD Biosciences, Mississauga, ON, Canada)]. All enzymatic digestions of testicular tissue were carried out in sterile glass dissociation flasks that were swirled in a 37°C water bath. Testicular tissue was enzymatically digested in the first enzyme solution for 25 min. 20 ml of DMEM/F12 containing 5% fetal bovine serum (FBS) was added to the flask to cease trypsin activities. Digested tissue was centrifuged at 800 rpm for 5 min at room temperature and the supernatant was removed, leaving a loose pellet. The pellet was then washed twice with 10 ml of washing solution (DMEM/F12 containing L-glutamine and antibiotics). After washing, the pellet was resuspended in 20 ml of the second enzyme solution [DMEM/F12 containing 2 mg/ml collagenase type I (Invitrogen, Burlington, ON, Canada), 2mg/ml hyaluronidase Type I-S (Sigma-Aldrich, Oakville, ON, Canada), 40 µg/ml crude deoxyribonuclease I (Sigma-Aldrich, Oakville, ON, Canada), 250 ng/ml fungizone, 100 U/ml penicillin and 0.1 mg/ml streptomycin, non-sterile components were sterilized with 0.20 µm pore size syringe filters (Corning Incorporated, Corning, NY, USA) and 10 ml syringes (BD Biosciences, Mississauga, ON, Canada)] and transferred to a new sterile dissociation flask. Testicular tissue was enzymatically digested for 35 min. No FBS treatment followed this second enzymatic digestion. Digested tissue was centrifuged at 600 rpm for 4 min at room temperature and the supernatant was removed, leaving a dense pellet. The pellet was then washed twice with 10 ml of washing solution. After washing, the pellet was resuspended in 20 ml of the final enzyme solution [Ca<sup>++</sup>-/Mg<sup>++</sup>-free

Dulbecco's Phosphate Buffered Saline (STEMCELL Technologies, Vancouver, BC, Canada) containing 0.5 mg/ml trypsin (STEMCELL Technologies, Vancouver, BC, Canada), 0.1 mg/ml EDTA (Fisher Scientific, Ottawa, ON, Canada), 4 mM dextrose (Fisher Scientific, Ottawa, ON, Canada), 250 ng/ml fungizone, 100 U/ml penicillin and 0.1 mg/ml streptomycin, non-sterile components were sterilized with 0.20 µm pore size syringe filters (Corning Incorporated, Corning, NY, USA) and 10 ml syringes (BD Biosciences, Mississauga, ON, Canada)] and transferred to a new sterile dissociation flask. Testicular tissue was enzymatically digested for 14 min. 20 ml of the 5% FBS solution was added to the flask to cease trypsin activities. Digested tissue was centrifuged at 800 rpm for 5 min at room temperature and the supernatant was removed, leaving a dense pellet. The pellet was then washed twice with 10 ml of washing solution. After washing, the pellet was resuspended in 5 ml of serum-free defined medium (SFDM). The cell suspension was diluted to a final concentration of  $>1.3 \times 10^6$  cells/0.2 ml SFDM. 0.2 ml of the final cell suspension was seeded onto the polymerized Matrigen™ layer inside cell culture inserts, and 0.8 ml SFDM was added to the wells of the cell culture plate. The cells were incubated at 34 °C with 5% CO<sub>2</sub>. Cell culture media were changed every two days.

A hypotonic wash solution was applied in place of SFDM to cultured cells two days after seeding to lyse contaminating germ cells. Debris from lysed germ cells was removed during subsequent media changes. The hypotonic wash solution was a 5 or 10 mM Tris-HCl (Sigma-Aldrich, Oakville, ON, Canada) solution at pH 7.50 [40, 52]. The hypotonic wash lasted for 2.5 min. After washing, the hypotonic wash solution was aspirated and replaced with SFDM. The cell culture plate was then gently shaken to loosen dead germ cells into SFDM. SFDM containing dead germ cells was aspirated again and was replaced with fresh SFDM.

Sertoli cells were cultured for seven days prior to being processed for fluorescence microscopy or electron microscopy.

### **Composition of serum-free defined medium (SFDM)**

SFDM was made by adding the following constituents to DMEM/F12 cell culture medium (Sigma-Aldrich, Oakville, ON, Canada) to obtain the indicated final concentrations [52]: 100 U/ml penicillin; 0.1 mg/ml streptomycin; 6.7 ng/ml sodium selenite (Invitrogen, Burlington, ON, Canada); 10 µg/ml insulin (Invitrogen, Burlington, ON, Canada); 5.5 µg/ml transferrin (Invitrogen, Burlington, ON, Canada); 250 ng/ml fungizone; 100 ng/ml recombinant human FSH (National Hormone & Peptide Program, Dr. A.F. Parlow, Torrance, CA, USA); 10 ng/ml recombinant human Epidermal Growth Factor (Sigma-Aldrich, Oakville, ON, Canada); 50 ng/ml Vitamin A (Sigma-Aldrich, Oakville, ON, Canada); 200 ng/ml vitamin E (Sigma-Aldrich, Oakville, ON, Canada);  $10^{-9}$  M hydrocortisone (Sigma-Aldrich, Oakville, ON, Canada);  $10^{-7}$  M testosterone (Sigma-Aldrich, Oakville, ON, Canada);  $10^{-8}$  M estradiol (Sigma-Aldrich, Oakville, ON, Canada); 2 mM L-glutamine (Invitrogen, Burlington, ON, Canada); 3 µg/ml cytosine beta-D-arabinofuranoside (Sigma-Aldrich, Oakville, ON, Canada).

### **Transfection of cultures with plasmids**

Cultured Sertoli cells were transfected with DNA plasmids encoding GFP-tagged claudin-11, GFP-tagged connexin-43 and GFP-tagged nectin-2 for two days prior to fixation. The plasmid for claudin-11 was constructed as indicated below, the plasmid for connexin-43 was generously provided by Dr. Naus (University of British Columbia) and the plasmid for nectin-2 was generously provided by Dr. Julian Guttman (Simon Fraser University). Lipofectamine™ 2000 (Invitrogen, Burlington, ON, Canada) was used as the transfection reagent. SFDM containing no antibiotics or antimycotics were used during transfection. For transfection of cells

in each cell culture insert designed for 24-well plates, 25  $\mu$ l SFDM were used to dilute DNA plasmid stock solutions, and 25  $\mu$ l SFDM were used to incubate Lipofectamine<sup>TM</sup> 2000 reagent for 10 min. 0.4  $\mu$ g of experimental DNA plasmid and 2  $\mu$ l of Lipofectamine<sup>TM</sup> 2000 were used in each cell culture insert (plasmid to transfection reagent w/v ratio = 1:5). The DNA plasmid and Lipofectamine<sup>TM</sup> 2000 solutions were mixed and allowed to incubate for 30 min, completing the transfection mix. During this incubation, regular SFDM in the cell culture plate was replaced with antibiotic-/antimycotic-free SFDM (50  $\mu$ l was added to inserts and 600  $\mu$ l was added to wells). After incubation, 50  $\mu$ l of the transfection mix was added to each cell culture according to the manufacturer's instructions. Cells were incubated at 34 °C with 5% CO<sub>2</sub> for at least 4 hrs prior to media change with normal SFDM.

Some cell cultures were transfected with the transfection agent alone or with empty vectors that do not contain fusion constructs (used at the same concentration as experimental fusion constructs) to serve as vehicle controls (Fig. 15, a and b). GFP-tagged junction protein fusion constructs were also transfected into the MDCK cell line to serve as positive controls (Fig. 13, f and g).

### **Construction of claudin-11-GFP plasmids**

Rat claudin-11 (Cldn11) was cloned from primary Sertoli cell cDNA into pcDNA3.1 and verified by DNA sequencing. To generate plasmid constructs expressing claudin-11 with N- or C-terminal EGFP fusions, two sets of oligonucleotide primers were designed, and used to amplify by PCR the claudin-11 coding region by using the rat claudin-11 cDNA clone as the template. I used primers 'A' and 'B' (sequence for forward primer 'A': CGAATTCGCCACCATGGTAGCCACTTGCCCTGCAG; sequence for reverse primer 'B':

GGGATCCCGGACATGGGCACTCTTGGCGTG) to clone the claudin-11 coding region that will be inserted into the pEGFP-N1 vector (Clontech Laboratories, Inc., Mountain View, CA, USA). I used primers 'C' and 'D' (sequence for forward primer 'C': CGAATTCGATGGTAGCCACTTGCCTGCAG; sequence for reverse primer 'D': GGGATCCTTAGACATGGGCACTCTTGG) to clone the claudin-11 coding region that will be inserted into the pEGFP-C1 vector (Clontech Laboratories, Inc., Mountain View, CA, USA). The PCR products were first cloned into pCR2.1-TOPO (Invitrogen, Burlington, ON, Canada), verified by restriction digestion (Fig. 16a) and DNA sequencing, and then sub-cloned into pEGFP-N1 and pEGFP-C1 to generate constructs expressing fusions of claudin-11 to the N- and C-termini of EGFP, respectively. These plasmid constructs were further verified by restriction digestion (Fig. 16b) and DNA sequencing. Prior to transfecting cultured Sertoli cells, the transfection efficacy of both types of plasmid constructs were experimentally verified in cultured MDCK cells. It was discovered that the pEGFP-N1 construct successfully transfected into MDCK cells and resulted in the production of green fluorescent signals that outlined the cell periphery (Fig. 13f), a characteristic of the localization behavior of claudin-11. The pEGFP-N1 construct was then selected for subsequent transfection into cultured Sertoli cells.

### **Immunofluorescence of Sertoli cell cultures**

Sertoli cells cultured for 7 days were fixed with 3% paraformaldehyde in PBS (150.0 mM NaCl, 4.0 mM Na/K PO<sub>4</sub>, 5.0 mM KCl, pH 7.30) for 30 min. After fixation, cells were washed 3 times with TPBS/BSA buffer (0.05% Tween 20 and 0.1% bovine serum albumin in PBS, pH 7.30). Whole filters were cut away from cell culture inserts with a scalpel and immediately submerged in cold acetone for 5 min to permeabilize cells. Following permeabilization, cells were further washed 3 times with TPBS/BSA buffer and blocked for 10 min with 5% normal

goat serum (NGS) (Sigma-Aldrich, Oakville, ON, Canada) or 5% normal donkey serum (NDS) (Sigma-Aldrich, Oakville, ON, Canada) in TPBS/BSA. Primary antibody solutions were then added to fixed cells and labeled at 4°C overnight. Cells were again washed with TPBS/BSA for a total of 3 times. Secondary antibody solutions were then added to cells and allowed to label for 1 hr at 37 °C. After incubation with secondary antibodies, cells were washed 3 times with TPBS/BSA. When needed, cells were stained with phalloidin after incubation with secondary antibodies. Whole filters were mounted on chromic acid-cleaned glass slides in VectaShield mounting medium with DAPI (Vector Laboratories, Burlington, ON, Canada) to stain for nuclei. Some filters were mounted in mounting medium without DAPI.

### **Immunofluorescence of tissue sections and tissue fragments**

Adult male Sprague-Dawley rats were anesthetized and testes removed. The testes were perfused briefly with PBS to clear blood from blood vessels, and then perfusion-fixed with 3% paraformaldehyde in PBS for 30 min then with PBS for 30 min.

For tissue sections [32], testes were mounted on stubs with Tissue-Tek<sup>®</sup> Optimal Cutting Temperature compound (Sakura Finetek USA, Torrance, CA) and quick-frozen in liquid nitrogen. 5 µm thick tissue sections were cut from testis with a cryo-microtome, and each was immediately transferred onto a glass slide coated with poly-L-Lysine (Sigma-Aldrich, Oakville, ON, Canada) and then submerged in cold acetone for 5 min.

For tissue fragments [32], testes were decapsulated and minced to a slurry. Minced testicular material was transferred to a 50 ml centrifuge tube (BD Biosciences, Mississauga, ON, Canada), passed through an eighteen gauge syringe needle and subsequently a twenty-one gauge needle to fragment the tissue and allowed to sediment by gravity. Fragmented tissue contained

within the resulting supernatant was transferred to a 15 ml centrifuge tube (BD Biosciences, Mississauga, ON, Canada) and centrifuged to separate Sertoli cells that remain attached to spermatids from free-floating cells. Subsequently, the supernatant was aspirated to remove free-floating cells, and the pellet was resuspended in buffer. A few drops of the resulting cell suspension were then applied to a poly-L-lysine-coated glass slide and immediately plunged into cold acetone for 5 minutes.

Slides were removed from acetone and allowed to air-dry. A water-repellent circle was drawn around each tissue section with a Liquid Blocker Super Pap Pen (Cedarlane, Burlington, ON, Canada) to retain liquids over the sections. 50 µl TPBS/BSA buffer containing 5% NGS or NDS were added to tissue sections as a blocking agent for 20 min. For sections only labeled for filamentous actin, 100 µl phalloidin stain were added in place of the blocking solution, directly followed by washing and mounting. After blocking, primary antibodies were applied to the slides and allowed to label at 4 °C overnight. After overnight incubation with primary antibodies, slides were washed three times with TPBS/BSA buffer. Secondary antibodies were applied to the slides and allowed to label for 1 hour at 37 °C. Slides were again washed three times with TPBS/BSA. Tissue sections or fragments that would be double-labeled for filamentous actin received phalloidin stain as a second wash following incubation with secondary antibodies. Water-repellent circles were removed with a razor blade. Tissue sections were mounted in VectaShield mounting medium with DAPI (Vector Laboratories, Burlington, ON, Canada) to stain for nuclei.

### **Antibodies and stains**

Primary antibodies were diluted with TPBS/BSA buffer containing 1% NGS. Primary antibodies from different host species were sometimes prepared together in a single solution to

double-label cells. Working concentrations of primary antibodies were as follows: polyclonal rabbit anti-Oligodendrocyte Specific Protein (anti-claudin-11) (Abcam, Cambridge, MA, USA; ab53041): 0.0025 mg/ml; monoclonal mouse anti-connexin-43 (Millipore, Etobicoke, ON, Canada; MAB3068): 0.0025 mg/ml; rabbit anti-nectin-2 was used at 1:500 dilution; polyclonal goat anti-GATA-4 (Santa Cruz Biotechnology, Santa Cruz, CA, USA; sc-1237): 0.0020 mg/ml; polyclonal rabbit anti-Rab5 (Abcam, Cambridge, MA, USA; ab13253): 0.0025 mg/ml or 0.00125 mg/ml; monoclonal mouse anti-alpha adaptin (anti-AP2) (Abcam, Cambridge, MA, USA; ab2807): 0.02 mg/ml; monoclonal rabbit anti-EEA1 (New England BioLabs, Pickering, ON, Canada; C45B10): 0.000315 mg/ml; monoclonal mouse anti-alpha smooth muscle Actin (Abcam, Cambridge, MA, USA; ab7817): 0.002 mg/ml; normal rabbit IgG (Jackson ImmunoResearch Laboratories, Inc., West Grove, PA, USA; 011-000-003), normal mouse IgG (Jackson ImmunoResearch Laboratories, Inc., West Grove, PA, USA; 015-000-003) and normal goat IgG (Sigma-Aldrich, Oakville, ON, Canada; I5256): diluted with PBS to a concentration of 1 mg/ml that served as the stock concentration, which was diluted to working concentrations based on concentrations of the experimental antibodies being controlled for; normal rabbit serum (Jackson ImmunoResearch Laboratories, Inc., West Grove, PA, USA; 011-000-120) was used at 1:500 dilution to control for rabbit anti-nectin-2.

Secondary antibodies were diluted with TPBS/BSA buffer to a working concentration of 0.02 mg/ml. Either Alexa Fluor<sup>®</sup> 568 Phalloidin or Alexa Fluor<sup>®</sup> 488 Phalloidin (Invitrogen, Burlington, ON, Canada; A12380 and A12379, respectively) was diluted 1:20 for cultured Sertoli cells and 1:5 or 1:2 for tissue sections with TPBS/BSA buffer.

### **Estimation of Sertoli cell culture purity by cell counting**

DAPI-stained nuclei of cells cultured in dual-compartment chambers were counted using the 'Cell Counter' plug-in for the ImageJ software. An antibody to alpha smooth muscle actin, which is a marker for peritubular myoid cells [59], was used to probe and allowed the counting of peritubular myoid cells. Fluorescent images were taken with a 40X objective on a conventional microscope. Cells already cultured in dual-compartment chambers were counted to obtain the most accurate results in an actual cell culture. Germ cells were recognized by their intensely-stained, small-sized and round nuclei. Peritubular myoid cells were recognized by their weakly-stained, large, stretched and oval-shaped nuclei. Sertoli cells were recognized by their intermediately-stained (weaker than germ cell nuclei but stronger than peritubular myoid cell nuclei), irregularly round nuclei (each of which has one or more 'dots' of more intense DAPI signal). Since Sertoli cell purity differs from area to area on a cell culture, a total of at least 1000 cells were counted for four of six separate experiments to improve estimation accuracy; less than 1000 cells were counted for the remaining two experiments because not enough cells were recorded in the images taken. For each of the six experiments, percentages of Sertoli cell purity were calculated as follows: the number of non-Seroli cells was divided by the total number of cells counted, then multiplied by 100%. The resulting percentage number was rounded upwards if digits after the decimal point were 0.45 or above, and downwards if the digits were 0.44 or below. This number was then subtracted from 100% to obtain the percentage of Sertoli cells among the cells counted. This method is not perfectly accurate and provides only an estimation to Sertoli cell culture purity.

A caveat to this approach is that at numerous times, cell nuclei were not optically focused and resulted in blurry DAPI signals, making it difficult to judge the cell type. To avoid counting less contaminant cells than the amount that was actually present, all uncertain cell types were

treated as contaminants. Furthermore, although peritubular myoid cells are counted using alpha smooth muscle actin signal, their DAPI-stained nuclei might not be visible in the optical plane at which the images were taken and were therefore not included in the total cell count. As a result, the actual Sertoli cell purity may be higher than what was calculated.

### **Electron Microscopy**

Tissue was processed for electron microscopy as described in detail elsewhere [60] except that isoflurane instead of halothane was used for anesthetizing the animals.

Primary Sertoli cell cultures were processed using the same fixatives and buffers as used for tissue. Media above and below the culture well insert membranes were replaced with fixative at room temperature and allowed to sit for 1 hr. The membrane was cut from the insert, transferred to a glass vial, and then immersion fixed for an additional 1.5 - 2 hrs. The membrane then was further processed in the same fashion as tissue.

Sections were evaluated and photographed on a FEI Tecnai G2 Spirit electron microscope operated at 120 kV.

### **3D analysis of confocal Z-stacks**

Fluorescent Z-stacks obtained with a Zeiss LSM 510 confocal microscope in the form of '.lsm' file types were imported into the Volocity software (PerkinElmer, Waltham, MA, USA). Each Z-stack was cropped in 'XYZ' mode along the X and Y axes to isolate the cell of interest and its immediate surroundings. The stack was further cropped along the Z axis to eliminate fluorescence that would otherwise obstruct viewing of the structure of interest three-dimensionally. The cropped stack was adjusted for brightness and contrast and a three-dimensional reconstruction was generated by viewing the stack in '3D Opacity' mode. Each 3D

image was further adjusted for brightness, density (transparency) and black level and subsequently rotated to produce optimal viewing of the structure of interest. To orient viewers, a spherical grid and indicators for X, Y and Z axes were also included. A snapshot of each 3D image was generated as a 2D image and exported as a TIFF file.

### **Analysis of junction staining**

An index of the amount of junction present at stages V and VII was determined by probing 5  $\mu\text{m}$  thick cryosections of seminiferous epithelium with phalloidin to label actin filaments in ectoplasmic specializations or with antibodies generated against claudin-11 to label tight junctions. A total of 13 tubules of each of Stage V and Stage VII were randomly chosen from sections of the testes of two different animals and photographed using identical exposures. Negatives were scanned into digital format and an area around the periphery of each tubule that contained only basal junction regions was selected. The areas in Stage V and Stage VII tubules were set to a predetermined threshold using ImageJ software [61]. The use of thresholding is an established technique [62-64] and have been used to test for differences between apical tubulobulbar complexes in control and cortactin knock-down testes [36]. When set to a common threshold, the number of positive pixels remaining above the threshold was determined using the ‘analyze particles’ function. The number of pixels was considered to be an index of the amount of junction present at basal junctions. A t-test was used to determine if the numbers of pixels above threshold were different between Stages V and VII.

## CHAPTER 3: RESULTS

### **Basal tubulobulbar complexes form within junction ‘pockets’**

In testis tissue processed for electron microscopy, basal junction complexes between neighboring Sertoli cells were identified at the ultrastructural level by the presence of unique adherens junctions termed ectoplasmic specializations. These structures consist of regions of a sub-membrane layer of close-packed actin filaments, and a cistern of endoplasmic reticulum (Fig. 2, a and b). Tight and gap junctions were present within the adhesion domains and were identified by the presence of membrane ‘kisses’ (Fig. 2, a and b) and closely opposed membranes respectively (Fig. 2a). Tubulobulbar complexes originated in zones of the cell occupied by ectoplasmic specializations (Fig. 2, c and d) and frequently appeared to be enclosed within ‘pockets’ or folds in the basal junction complexes (Fig. 2, c, d and f).

### **Basal tubulobulbar complexes contain morphologically identifiable intercellular junctions**

As shown previously by others [28], basal tubulobulbar complexes were observed to have all the features of apical complexes that occur between Sertoli cells and spermatids; that is, each complex had a long proximal tubule cuffed by an actin network and the entire structure was capped by a coated pit that retained a connection to the adjacent cell. Unlike apical complexes, the tip of the adjacent cell did not have a density associated with the plasma membrane attached to the pit (Fig. 2e). Large bulbs or swellings developed in the distal third of the complexes and were closely related to cisternae of endoplasmic reticulum (Fig. 2, f and g). Significantly, tight and gap junctions, recognized by the presence of membrane kisses and closely opposed membranes similar to those found within junction complexes, were identified both in tubular regions of the complexes (Fig. 2, h and i) and in the bulbs (Fig. 2, f, g, j and k).

These results confirm Russell's [29] report that ultrastructurally identifiable tight and gap junctions are present in basal tubulobulbar complexes.

### **Basal tubulobulbar complexes contain claudin-11, connexin-43 and nectin-2**

In cryo-sections of perfusion fixed testis double-labeled for filamentous actin and claudin-11, connexin-43 or nectin-2, rod-like protrusions were identified extending away from the Sertoli cell junction complexes that formed intense linear bands of fluorescence near the base of the epithelium. These protrusions were positive both for junction proteins as well as for actin (Fig. 3, a to i). Signal strengths of junction protein staining were well above those of non-specific staining (Fig. 3, c, f, i and their respective insets).

I conclude that basal tubulobulbar complexes in the seminiferous epithelium contain tight, gap and adhesion junction proteins.

### **The endocytic markers EEA1 (early endosome antigen 1) and Rab5 associate with basal tubulobulbar complexes**

To determine if markers for early endosomes labeled regions known to contain tubulobulbar complexes, I probed cryo-sections of perfusion fixed testis with antibodies against filamentous actin and EEA1, or for connexin-43 and EEA1. Staining for EEA1 often occurred within fluorescent 'pockets' within the basal junction complex labeled for filamentous actin (Fig. 4, a and b) or connexin-43 (Fig. 4, c and d). EEA1 signals also were observed to cap the ends of rod-like protrusions that extend from junction 'bands' (Fig. 4e) and resemble what were seen at apical tubulobulbar complexes (lower inset in Fig. 4e). When sections were labeled for Rab5 and

connexin-43 or actin, staining for Rab5 occurred near or at the tips of linear structures labeled for connexin-43 (Fig. 4f) or actin (Fig. 4g) similar to what occurs at apical tubulobulbar complexes (inset in Fig. 4g) [33]. Non-specific staining was virtually non-existent when compared to EEA1 or Rab5 staining (insets of Fig. 4, e and f, respectively).

I have also attempted to confirm *in vivo* observations by immunoprobng EEA1 and Rab5 in cultured Sertoli cells. Observations similar to those from *in vivo* samples were made where EEA1 (Fig. 14, a and b) or Rab5 (Fig. 14, d and e) signals occurred near or at the tips of rod-like protrusions positive for connexin-43 signal. However, in cultured Sertoli cells, signal strengths and staining patterns of EEA1 and Rab5 were not significantly different from those of non-specific staining (Fig. 14, c and f) and therefore cannot fully confirm the *in vivo* results.

I conclude that basal tubulobulbar complexes are associated with markers for early events in the endocytosis pathway.

### **Basal junctions are less apparent after the peak appearance of tubulobulbar complexes**

Basal tubulobulbar complexes tend to peak in their formation at Stages IV-V of spermatogenesis in rat and degrade during Stages VI-VII [29]. If tubulobulbar complexes are involved with internalization of junctions, then junction complexes should be less apparent at stage VII after junctions have been internalized and degraded than at Stages IV-V when tubulobulbar complexes are most apparent in the epithelium. This was the case when cryo-sections of perfusion fixed testis were stained for ectoplasmic specializations with a probe for actin (Fig. 5, a and b) and also was the case when similar sections were stained for tight junctions with a probe for claudin-11 (Fig. 6, a and b).

I conclude that junctions are being reduced in size or are being degraded prior to the actual beginning of spermatocyte translocation in Stages VIII-IX of spermatogenesis, and that this reduction correlates temporally with the time over which tubulobulbar complexes are most easily detected in the epithelium [29].

### **Basal tubulobulbar complexes form in primary cultures of rat Sertoli cells**

To explore the possibility of developing an *in vitro* model system that would enable easy manipulation for doing detailed experimental studies, for better resolving structure at the light level, and for doing live cell imaging, I evaluated primary Sertoli cell cultures for the presence of tubulobulbar complexes.

Sertoli cell cultures were established by me as described in the Materials and Methods. To verify that, in my hands, primary cultures of Sertoli cells morphologically differentiate as reported by others [49, 50, 52], I evaluated my cultures for cell shape, nuclear position and the presence of cell specific basal junction complexes.

In my cultures, Sertoli cells established and maintained a morphologically differentiated phenotype that varied from low to high columnar depending on position in the culture insert and how extensively the cells were able to mechanically manipulate the Matrigel<sup>TM</sup> on which they were plated. The more columnar cells extended processes into the underlying matrix layer that appeared thicker in these regions than in areas where the cells were more cuboidal (Fig. 7, a to d). The nuclei of the cells were present at their bases, similar to what is observed in the intact seminiferous epithelium.

When observed at the ultrastructural level, junction complexes, identified by the presence of ectoplasmic specializations, occurred near the base of the monolayer between neighboring

Sertoli cells (Fig. 7e). Membrane kisses, indicative of tight junctions, were present within the junction complexes (Fig. 7, f and g).

Significantly, when observed by electron microscopy, tubulobulbar complexes were present between neighboring Sertoli cells in regions of intercellular contact (Fig. 8, a and b). These structures were identified by their tubular appearance, their double membrane core and their cuff of actin filaments arranged in a network. The plasma membrane of the adjacent cell attached to the coated pit at the tip of each complex lacked a sub-membrane density (Fig. 8c); this is also a characteristic of basal tubulobulbar complexes found in the intact epithelium (see Fig. 2e), and is different than apical tubulobulbar complexes that have a density associated with the spermatid plasma membrane. In addition to more mature complexes, double-membrane coated pits and tubulobulbar complexes in the early stages of formation were observed at ectoplasmic specializations (Fig. 8, d to g). Like in the intact seminiferous epithelium, tubulobulbar complexes in primary cultures of Sertoli cells occasionally were observed within pockets or folds in basal junction complexes (Fig. 9a).

Tubulobulbar complexes in primary cultures were oriented either perpendicular (Fig. 9, b and c) or parallel (Fig. 9, d and e) to the cell periphery. In all cases, the structures had a coated pit at their tip (arrowheads in Fig. 9, a to e) and formed from sites at the periphery of the cells where components of ectoplasmic specializations could be identified (arrows in Fig. 9, b, c and d).

Unlike *in vivo*, basal tubulobulbar complexes in the primary Sertoli cell cultures did not develop large bulbs in distal regions, although enlarged regions and ectopic swellings associated with elements of endoplasmic reticulum were occasionally observed (asterisks in Fig. 9, c and e).

It should be noted that both basal junction complexes and basal tubulobulbar complexes can be observed in low columnar as well as high columnar cells. A quantitative comparison of the exact amounts of the basal structures that are present in these cells, however, was not performed in the present study.

### **Tubulobulbar complexes *in vitro* contain morphologically identifiable junctions**

Similar to basal tubulobulbar complexes that form between Sertoli cells *in vivo*, high resolution electron microscopic evaluation of tubulobulbar complexes formed *in vitro* revealed that they contained membrane kisses indicative of the presence of tight junctions (arrowheads in Fig. 10, a, b and c).

### **Tubulobulbar complexes in primary Sertoli cell cultures contain junction proteins**

To further explore the possibility that the tubulobulbar complexes formed in primary Sertoli cell cultures contain junction proteins, primary cultures were probed for filamentous actin and for nectin-2 (Fig. 11, a to d), claudin-11 (Fig. 11, e to h) and connexin-43 (Fig. 11, i to l). All immunological probes outlined the periphery of Sertoli cells in regions known to contain basal junction complexes. Significantly, rod-like protrusions that were positive for junction proteins as well as for filamentous actin were observed to arise from the cell periphery and extend into the cells (arrowheads in Fig. 11). These linear protrusions resembled similar structures observed *in vivo* and were consistent with the tubulobulbar complexes observed at the ultrastructural level. When Z-stacks obtained with a confocal microscope were analyzed in three dimensions using the Volocity software (PerkinElmer, Waltham, MA, USA), these linear protrusions were verified to be tubular in nature (Fig. 11, d, h and l).

To verify that basal tubulobulbar complexes contain junction proteins *in vitro*, the clathrin related protein AP2 was used as an additional marker for tubulobulbar complexes. AP2 is a heterotetramer adaptor that facilitates clathrin coat assembly on the cell membrane and can be localized between the clathrin coat and the cell membrane [65, 66]. Since clathrin is known to be present at the tips of tubulobulbar complexes [67], AP2 would localize to the same position. When labeled for AP2, staining occurred either at or near the ends of junction positive tubules (Fig. 12, a to e), thereby confirming that the linear structures were likely tubulobulbar complexes that contain junction proteins.

Signal strengths of AP2 and nectin-2 staining were well above those of non-specific staining (insets in Fig. 12, a and d).

### **Junction proteins from one Sertoli cell are internalized by neighboring Sertoli cells**

To verify that junction proteins from one Sertoli cell are internalized into a neighboring Sertoli cell as predicted by the junction internalization hypothesis, cultured Sertoli cells were transfected with DNA plasmids that contain sequences encoding GFP-tagged junction proteins (claudin-11, connexin-43 and nectin-2). Cells were stained with an antibody targeting GATA-4 as a somatic cell marker to immunoprobe for Sertoli cell nuclei (Fig. 13, a-e), and some cells also were stained with AP2 (Fig. 13d) or filamentous actin (Fig. 13e). Transfection efficiency in primary Sertoli cell cultures was extremely low with only a few transfected Sertoli cells present in each culture. As a result, transfected Sertoli cells were surrounded by a pool of neighboring non-transfected, GATA-4-positive Sertoli cells. As predicted, fluorescence from junction-protein-GFP primarily localized to the periphery and to some degree to the cytoplasm of transfected cells. Significantly, rod-like protrusions projected into neighboring non-transfected

cells that were otherwise devoid of green fluorescent signal (Fig. 13, a and b). In other instances, GFP-positive vesicles were observed in non-transfected Sertoli cells that neighbored transfected ones (Fig. 13c). GFP-positive vesicles that were observed in non-transfected cells also were associated with AP2 (Fig. 13d) or rod-like protrusions positive for filamentous actin that extend from the cell periphery (Fig. 13e). The presence of junction-protein-GFP signals in Sertoli cells that were not transfected suggests that the tagged junction proteins were being internalized by neighboring cells. I was unable to convincingly demonstrate the presence of endocytic markers associated with the tubulobulbar complexes because of excessive background staining.

Vehicle controls revealed that the transfection reagent and empty vectors alone did not produce the observed GFP signal patterns (Fig. 15, a and b). Specificity controls revealed that the experimental nuclear and junction protein staining were not non-specific (Fig. 15, c and d). Positive controls revealed that when transfected into the readily proliferative MDCK cell line, my GFP-tagged claudin-11 fusion construct as well as the GFP-tagged nectin-2 fusion construct were indeed functional in an *in vitro* setting (Fig. 13, f and g). In the positive controls, GFP signals localized to the cell periphery where intercellular junctions would be present.

### **Sertoli cell cultures are approximately 85% pure**

To assess the level of contamination from non-Sertoli cells (such as germ cells and peritubular myoid cells) in a Sertoli cell-enriched culture, cells from six separate experiments were counted, and results are as follows (percentages were approximate): out of 1002 cells counted, 86% were Sertoli cells and 7% were peritubular myoid cells; out of 684 cells counted, 88% were Sertoli cells and 5% were peritubular myoid cells; out of 467 cells counted, 79% were Sertoli cells and 4% were peritubular myoid cells; out of 1194 cells counted, 86% were Sertoli

cells and 3% were peritubular myoid cells; out of 1057 cells counted, 77% were Sertoli cells and 8% were peritubular myoid cells; out of 1172 cells counted, 86% were Sertoli cells and 10% were peritubular myoid cells. Taken together, the average purity of primary Sertoli cell cultures in my hands is approximately 85%.

## CHAPTER 4: DISCUSSION

In this study I present evidence consistent with the conclusion that tubulobulbar complexes that form at basal sites in the seminiferous epithelium are sub-cellular machines that internalize intercellular junctions into one or the other of the attached Sertoli cells. Also, I show that tubulobulbar complexes develop in primary cultures of Sertoli cells. The results have implications for the mechanism by which spermatocytes translocate through the blood-testis barrier during spermatogenesis, and for future *in vitro* studies of junction remodeling by Sertoli cells.

Tubulobulbar complexes are elongate structures that develop at sites of intercellular attachment in the seminiferous epithelium [28]. Each complex consists of a tubular core, formed by the two attached membranes of adjacent cells, which is cuffed by a dendritic network of actin filaments [67]. The entire structure is capped at its end by a clathrin-coated pit [67]. Distal regions of the complex swell and eventually separate from the complex to be internalized and degraded by the Sertoli cell [68]. There is a growing body of evidence that tubulobulbar complexes that form at apical sites of attachment between Sertoli cells and spermatids internalize adhesion junctions. The structures contain intercellular adhesion proteins and are associated with endocytic markers [31-33]. Moreover, disruption of apical tubulobulbar complexes or their failure to form is correlated with spermiation delay or failure [34-36] – a phenotype predicted on the basis of the junction internalization hypothesis.

### **The role of basal tubulobulbar complexes in junction internalization**

Tubulobulbar complexes that form at intercellular junctions near the base of the epithelium between neighboring Sertoli cells resemble those complexes present at apical sites

[28], and data presented here are consistent with a role in junction internalization. Morphologically recognizable tight and gap junctions were identified in the structures by Russell in his original work on tubulobulbar complexes [29], and these results have been confirmed in the present study. In addition, putative basal complexes label with antibodies raised against components of all three major junction types (adhesion – nectin-2, tight – claudin-11 and gap – connexin-43) when evaluated by fluorescence microscopy. In the latter immunofluorescence studies, the observation that the ends of the tubular structures are positive for the clathrin related protein AP2 is consistent with the conclusion that the structures are indeed tubulobulbar complexes. Moreover, early endocytosis markers are found in similar locations as basal tubulobulbar complexes, and in some cases have the same staining pattern as those associated with apical tubulobulbar complexes [32, 33]. These results together strongly support the conclusion that basal tubulobulbar complexes likely internalize junctions. Significantly, the ultrastructural data from conventional transmission electron microscopy indicate that junction proteins in adjacent membranes do not entirely disengage from each other prior to being incorporated into tubulobulbar complexes. Although junction proteins can remain attached to each other as they are incorporated into tubulobulbar complexes, freeze fracture images of double-membrane vesicles in Sertoli cells presented by others [69] suggest that the junctions likely become fragmented laterally within the plane of the membrane and therefore no longer contribute functionally to basal junction complexes or to the blood-testis barrier.

The conclusion that junction proteins from one Sertoli cell are internalized together with junction proteins from the adjacent Sertoli cell by tubulobulbar complexes not only is consistent with ultrastructural findings, but is consistent with data from my *in vitro* studies where GFP-tagged proteins in transfected cells associate with markers for tubulobulbar complexes and

protrude into and are internalized by the adjacent non-transfected cells that are otherwise devoid of GFP signals.

A schematic diagram showing the proposed mode of formation of a basal tubulobulbar complex and how it internalizes basal junctions is depicted in Fig. 17.

### **Tubulobulbar complexes in the *in vitro* system**

As far as I know, this is the first study to report that tubulobulbar complexes form in morphologically differentiated primary cultures of Sertoli cells. Primary cultures have been used to study Sertoli cell structure and function for many years [37-48]. Of particular significance has been the use of inserts together with matrix and hormones to enable the cells to morphologically differentiate [39, 49-52]. Although these primary cultures have been used extensively to study intercellular junctions, the presence of tubulobulbar complexes in these systems has not been demonstrated.

Here I show that the tubulobulbar complexes that develop in primary culture are tubular in nature, are composed of the attached plasma membranes of two adjacent Sertoli cells, form in association with basal junction complexes, are capped by coated pits, are cuffed by an actin network, and can occur in folds or pockets in basal junctions. Moreover, like their *in vivo* counterparts, the structures contain ultrastructurally identifiable junctions and also label positively for junction proteins by immunofluorescence microscopy. One interesting feature of the complexes that form in culture is that they fail to develop the large terminal ‘bulbs’ characteristic of the complexes *in vivo*, although some of the structures do enlarge near their ends and are somewhat related to cisternae of endoplasmic reticulum. The failure to develop fully mature bulbs may indicate that the culture system does not completely replicate *in vivo*

conditions. This is consistent with my observation that I could not confirm the localization of endocytic markers in culture. One obvious missing feature of the culture system is the absence of the complex somatic/germ cell interactions that occur in the fully intact seminiferous epithelium.

Our novel finding that tubulobulbar complexes form in primary cultures of Sertoli cells indicates that basal tubulobulbar complexes may be involved with constitutive junction turnover in Sertoli cells – a conclusion consistent with the observation that basal tubulobulbar complexes are present at all Stages of the cycle of the seminiferous epithelium *in vivo* [29]. Importantly, formation of tubulobulbar complexes in primary Sertoli cell cultures provides an *in vitro* model system for studying the control of tubulobulbar complexes and their role in junction remodeling.

### **The role of basal tubulobulbar complexes in spermatocyte translocation**

The report that basal tubulobulbar complex formation dramatically peaks at Stages IV-V in the rat seminiferous epithelium [29] has renewed significance when viewed within the context of junction remodeling relative to spermatocyte translocation from basal to adluminal compartments during Stages VIII-IX. Basal junction remodeling appears to begin much earlier than the actual physical translocation of spermatocytes through the junctions, and much earlier than previously appreciated. My observation that there is considerably less junction (actin in ectoplasmic specializations, and claudin-11 in tight junctions) present at Stage VII than at Stage V, and that the difference in pixels remaining above threshold between the two stages is statistically significant, is consistent with the hypothesis that tubulobulbar complexes internalize junctions. The temporal separation of peak tubulobulbar complex formation and physical translocation of spermatocytes [29] indicates that junction remodeling related to spermatocyte translocation may be a multi-step process, beginning with a reduction in the amount of ‘junction’

present through the action of tubulobulbar complexes that begins well before Stage VIII, the upward movement of spermatocytes starting in Stage VIII, the formation of new junctions inferior to the translocating spermatocytes beginning in Stage VIII, and the final disassembly of junctions (possibly by tubulobulbar complexes) above the spermatocytes eventually leading to their entry into the adluminal compartment. This is different from the canonical model of spermatocyte translocation proposed by Russell [25] that simply involves un-zippering of junctions above and the re-formation of new junctions below the translocating spermatocytes.

Significantly, the fact that the peak formation of tubulobulbar complexes at basal sites precedes that at apical sites indicates that junction remodeling associated with spermatocyte translocation actually begins prior to that associated with spermiation. This has implications for current models of the interaction between these two events [70]. It also is interesting that the peak in basal tubulobulbar complex formation occurs at roughly the same stages of spermatogenesis where elongate spermatids are moved to their deepest point in the epithelium. Any functional inter-relationship between entrenchment of spermatids and basal junction remodeling remains to be determined.

Unlike at apical sites where a link between tubulobulbar complex formation and spermiation has now been fairly well established, the link between the function of tubulobulbar complexes and spermatocyte translocation at basal sites is less substantiated. If tubulobulbar complexes are indeed related to junction restructuring associated with spermatocyte translocation, then disruption of basal tubulobulbar complexes should compromise spermatocyte translocation. This prediction has not yet been verified experimentally.

## Overview of conclusions

I conclude that tubulobulbar complexes that form in areas of contact between Sertoli cells in basal regions of the seminiferous epithelium internalize elements of the basal junction complex. My results are consistent with the 'junction internalization hypothesis' of tubulobulbar complex function generally in the seminiferous epithelium, and add a new dimension to our understanding of basal junction remodeling in the seminiferous epithelium as it relates to spermatocyte translocation. My study also provides a valuable model system for studying the process of junction remodeling *in vitro*.

## CHAPTER 5: FIGURES

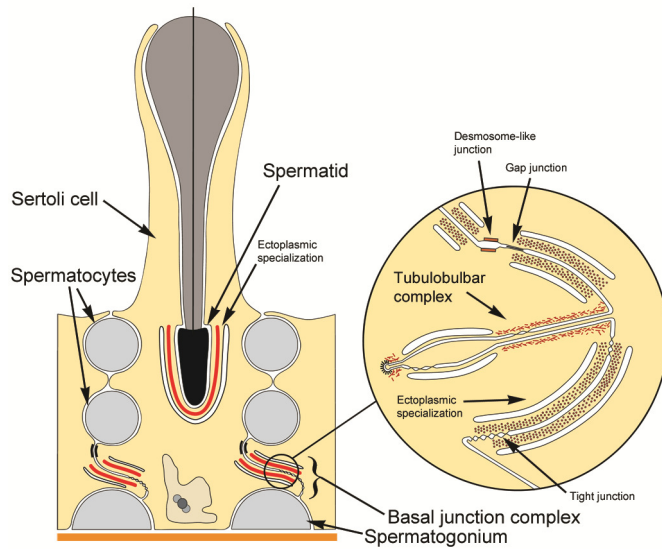


FIG. 1. Schematic diagram of a tubulobulbar complex and seminiferous epithelium. Shown here is a schematic diagram of a section through the seminiferous epithelium showing the positions of tubulobulbar complexes and of basal junctions between Sertoli cells.

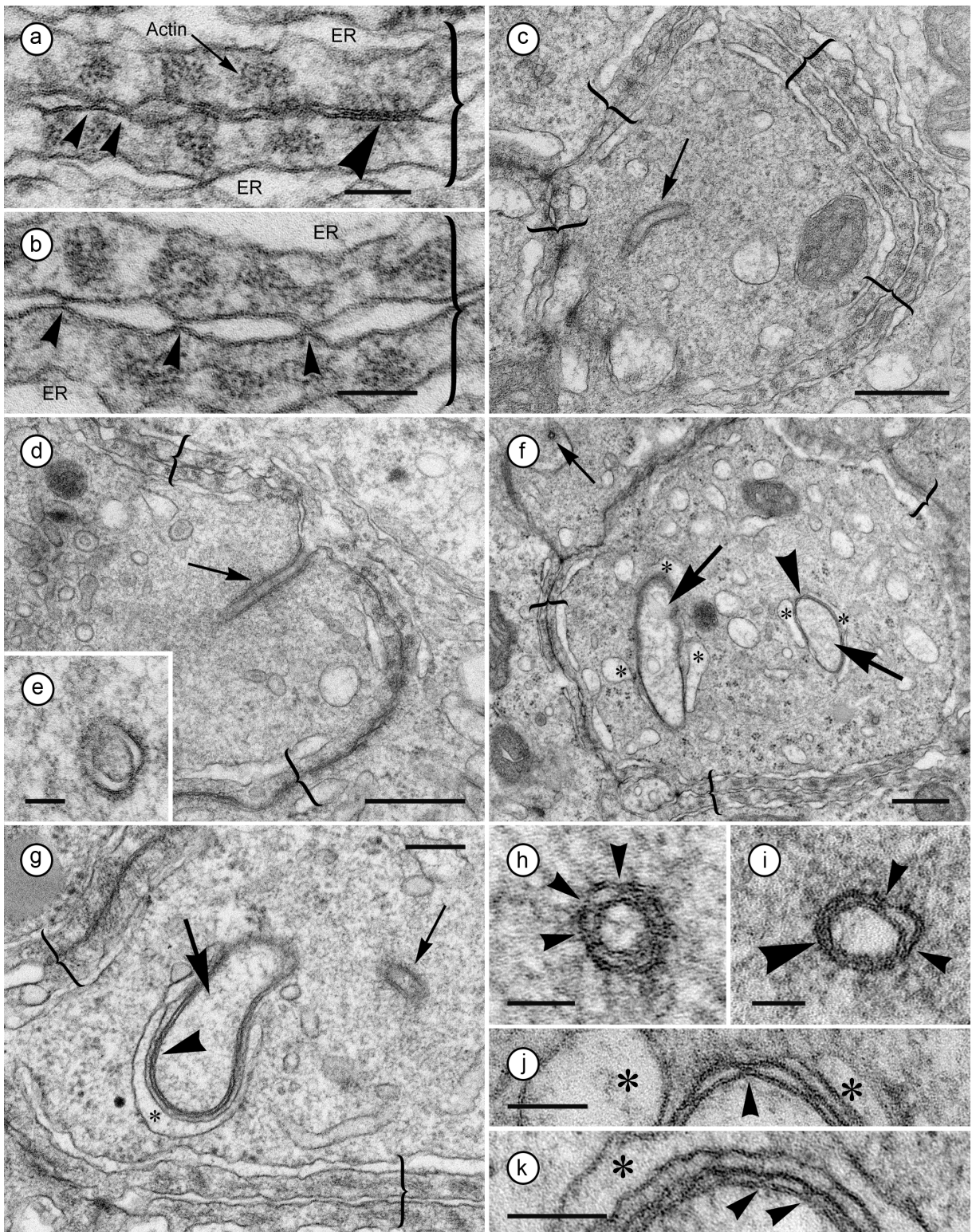


FIG. 2. Electron micrographs of basal junction complexes between Sertoli cells and associated tubulobulbar complexes. (a,b) Basal junction complexes (brackets) between Sertoli cells. Tight junctions are indicated by the small arrowheads. The large arrowhead in (a) indicates a gap

junction. Bars = 100 nm. (c,d) Proximal tubules (arrows) of tubulobulbar complexes are often within pockets or folds in basal junction complexes. Junction complexes are indicated by the brackets. Bars = 500 nm. (e) Cross section of a coated pit at the end of a tubulobulbar complex. Bar = 100 nm. (f,g) Bulb regions (large arrows) of tubulobulbar complexes. The asterisks indicate associated cisternae of endoplasmic reticulum. The small arrows indicate proximal tubular regions of tubulobulbar complexes and the arrowheads indicate the presence of junction elements in the bulbs. The arrowhead in (f) is shown at higher magnification in (j). (f) Bar = 500 nm, (g) Bar = 200 nm. (h,i) Cross sections through the proximal tubular regions of tubulobulbar complexes showing the presence of tight junctions (arrowheads) similar to those identified at junction complexes in (a) and (b). A gap junction is indicated by the large arrowhead in (i). Bars = 50 nm. (j,k) Sections through bulbs of two tubulobulbar complexes that document the presence of tight junctions (arrowheads) in the structures. The asterisks indicate cisternae of endoplasmic reticulum. Bars = 100 nm.

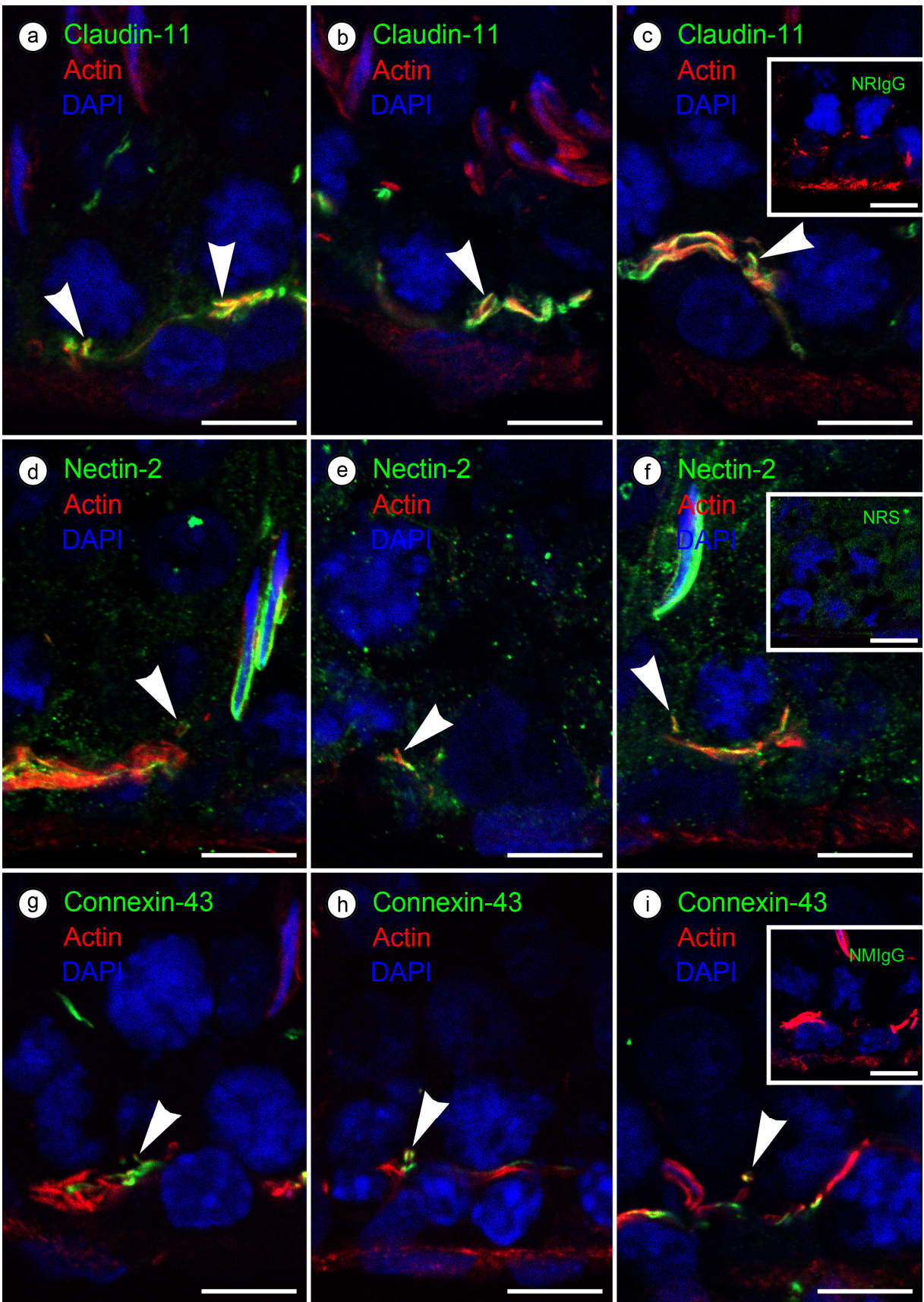


FIG. 3. Confocal images of putative basal tubulobulbar complexes in cryo-sections of adult rat seminiferous epithelia approximately at Stage V of spermatogenesis. Filamentous actin was stained with phalloidin (red color) and used as a marker for tubulobulbar complexes. Nuclei of spermatids, spermatocytes and Sertoli cells were stained with DAPI (blue color). Putative basal tubulobulbar complexes appear as relatively short rod-like protrusions (arrowheads) that extend away from 'threads' or 'bands' of basal junctions in the epithelium. Both filamentous actin and junction proteins (green color) localize to the same rod-like structures, suggesting that putative basal tubulobulbar complexes contain junction proteins. (a,b,c) Rod-like structures immuno-reactive for the tight junction protein claudin-11. A rod-like structure appears to occur within a junction 'pocket' in (c). (d,e,f) Rod-like structures immuno-reactive for the adhesion junction protein nectin-2. (g,h,i) Rod-like structures immuno-positive for the gap junction protein connexin-43. (i) Connexin-43 staining localizes to the end region of a rod-like structure, the body of which contains filamentous actin. Insets in (c,f,i) show normal IgG or serum controls in sections of seminiferous epithelia. Normal rabbit IgG (NRIgG), normal rabbit serum (NRS) and normal mouse IgG (NMIgG) were used to control for staining of claudin-11, nectin-2 and connexin-43, respectively. Insets in (c,i) have actin staining (red color) whereas the inset in (f) does not. Bars = 10  $\mu$ m.

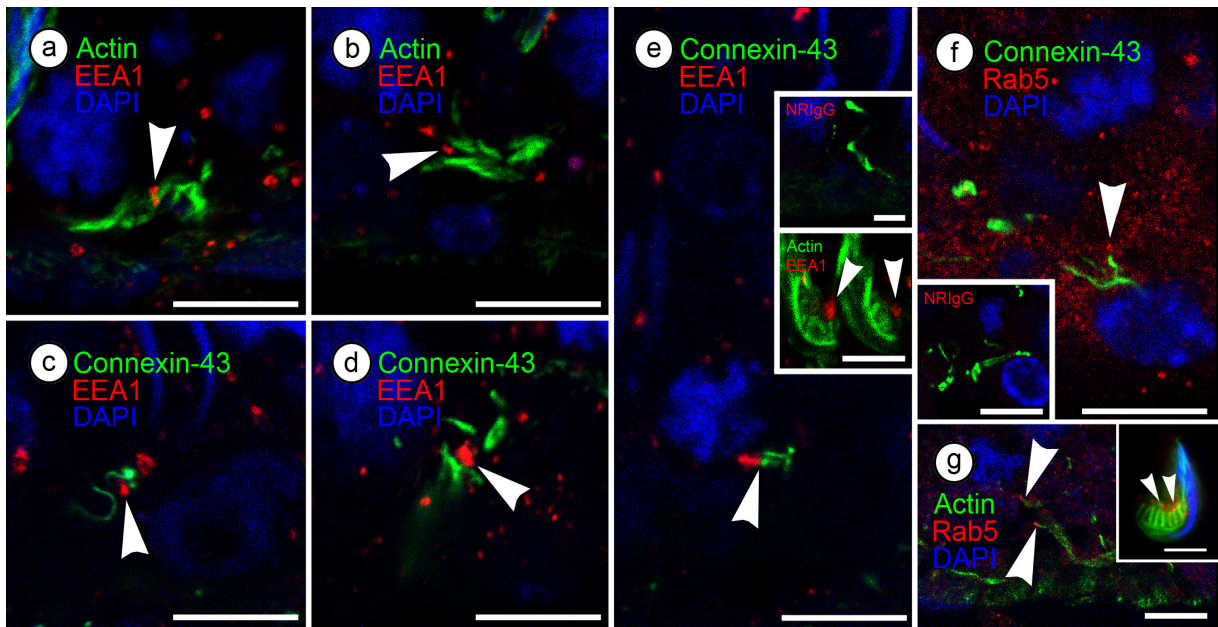


FIG. 4. Confocal images of basal junction regions in adult rat seminiferous epithelia immunoprobed for endocytic markers EEA1 (early endosome antigen 1) and Rab5. Junction bands or lines often form junction ‘pockets’ and putative basal tubulobulbar complexes frequently form within these junction pockets or folds. (a) Prominent EEA1 immunofluorescent signal (arrowhead) is seen within a junction pocket or fold. (b) Prominent EEA1 signal (arrowhead) within a portion of a junction pocket formed by actin filament bundles in ectoplasmic specializations. (c,d) Prominent EEA1 signals within portions of junction pocket formed by gap junctions (arrowheads). (e) EEA1 signal caps the end of a rod-like protrusion (arrowhead) that extends away from gap junctions. Lower inset in (e) shows actin-positive tubulobulbar complexes at apical sites of attachment between a Sertoli cell and a spermatid similarly capped by EEA1 signals (arrowheads). (f) Rab5 signal is present near the end of a rod-like protrusion (arrowhead) that extends away from gap junctions. (g) Rab5 signals cap the ends of two rod-like protrusions (arrowheads) that extend away from ectoplasmic specializations. The rod-like protrusions are likely basal tubulobulbar complexes. Inset in (g) shows similarly stained apical tubulobulbar complexes (arrowhead) imaged with conventional fluorescence microscopy. Upper inset in (e) and inset in (f) show normal rabbit IgG (NR1gG) controls in sections of

seminiferous epithelia for the staining of EEA1 (upper inset in e) or Rab5 (inset in f). The normal IgG controls were double-labeled for connexin-43 (green color). (a-g) Bars = 10  $\mu\text{m}$ . Bar in inset in (f) = 10  $\mu\text{m}$ . Bars in insets in (e,g) = 5  $\mu\text{m}$ .

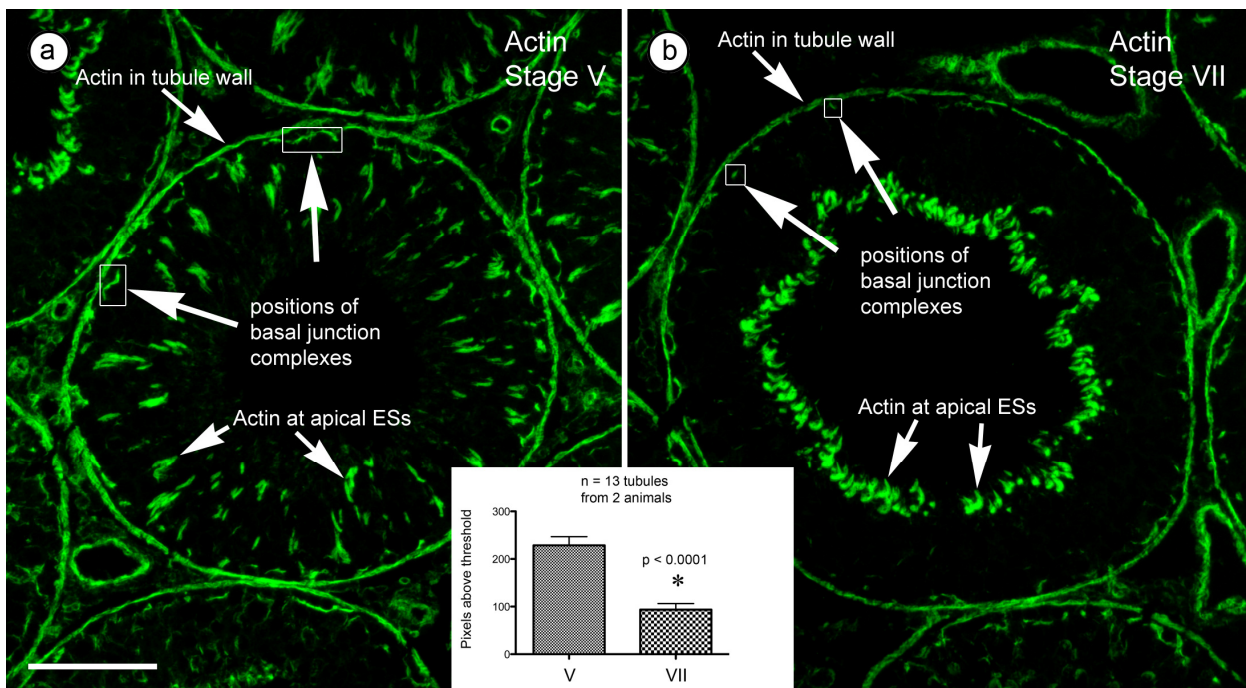


FIG. 5. Conventional immunofluorescence images of 5  $\mu\text{m}$  thick cryo-sections from perfusion fixed rat testis labeled for actin at approximately Stage V (a) and Stage VII (b) of the cycle of the seminiferous epithelium. (a,b) Actin labels the tubule wall as well as apical ectoplasmic specializations (apical ESs) at the Sertoli cell-spermatid interface and can be used to identify Stages V and VII. At Stage V, elongate spermatid heads are deep within apical Sertoli cell crypts. At Stage VII, late spermatid heads are at the apex of the epithelium, are hook-shaped and have a prominent lobule of Sertoli cell cytoplasm adjacent to their concave face. Examples of basal junctions (green fluorescence) as seen in a section through a single seminiferous tubule are indicated by the arrows that point to the boxes. The orientation of basal junctions is roughly parallel to the tubule wall, as schematically indicated in Fig. 1. The bar graph inset indicates the

numbers of pixels specifically in junction regions above an arbitrary threshold for tubules at Stage V and Stage VII and serves as an index of the amount of ectoplasmic specialization present at each of the stages. Bar = 0.1 mm.

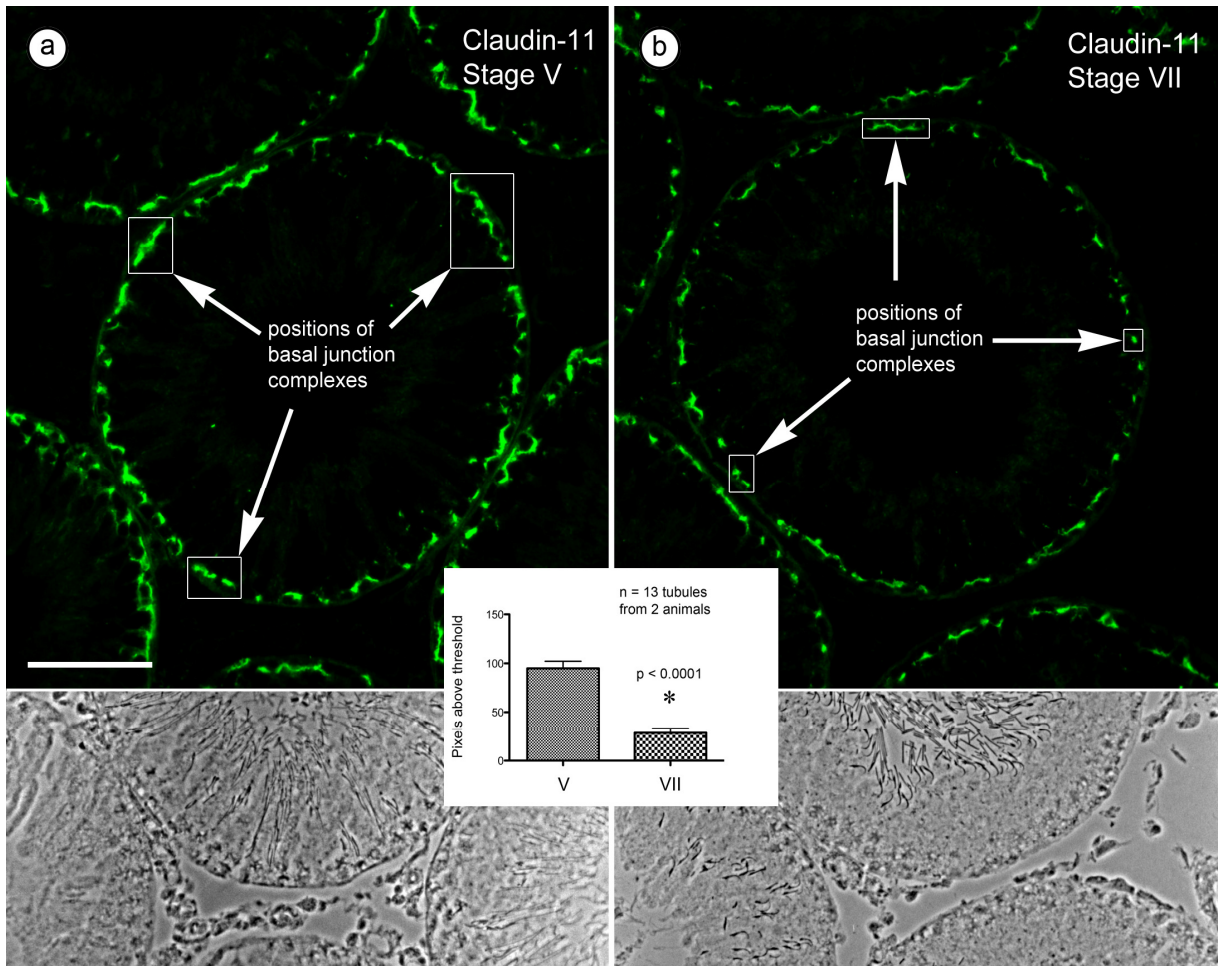


FIG. 6. Conventional immunofluorescence images of 5  $\mu$ m thick cryo-sections from perfusion fixed rat testis labeled for claudin-11 at approximately Stage V (a) and Stage VII (b) of the cycle of the seminiferous epithelium. (a,b) At Stage V, elongate spermatid heads are deep within apical Sertoli cell crypts. At Stage VII, late spermatid heads are at the apex of the epithelium, are hook-shaped and have a prominent lobule of Sertoli cell cytoplasm adjacent to their concave face. Examples of basal junctions (green fluorescence) as seen in a section through a single

seminiferous tubule are indicated by the arrows that point to the boxes. The orientation of basal junctions is roughly parallel to the tubule wall, as schematically indicated in Fig. 1. The corresponding phase images at the bottom of the panels verify stages in the fluorescence images above. The bar graph inset indicates the numbers of pixels specifically in junction regions above an arbitrary threshold for tubules at Stage V and Stage VII and serves as an index of tight junction amount present at each of the stages. Bar = 0.1 mm.

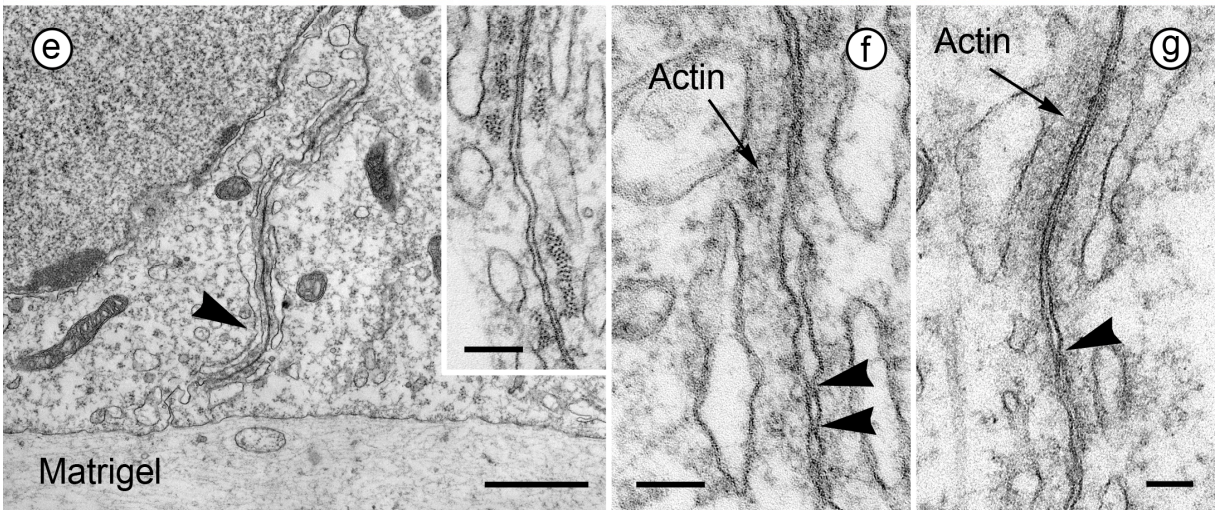
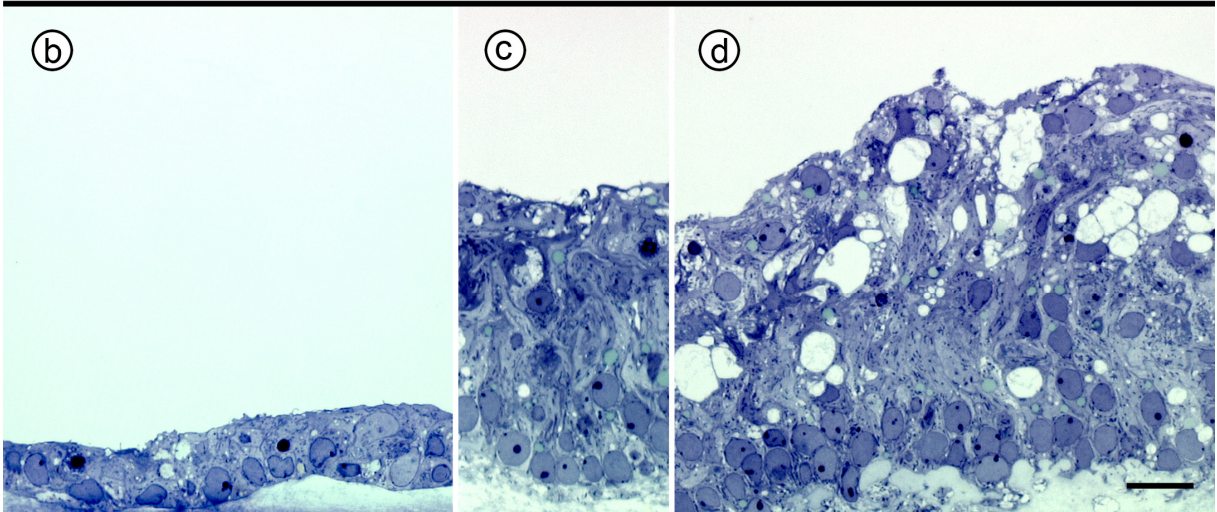
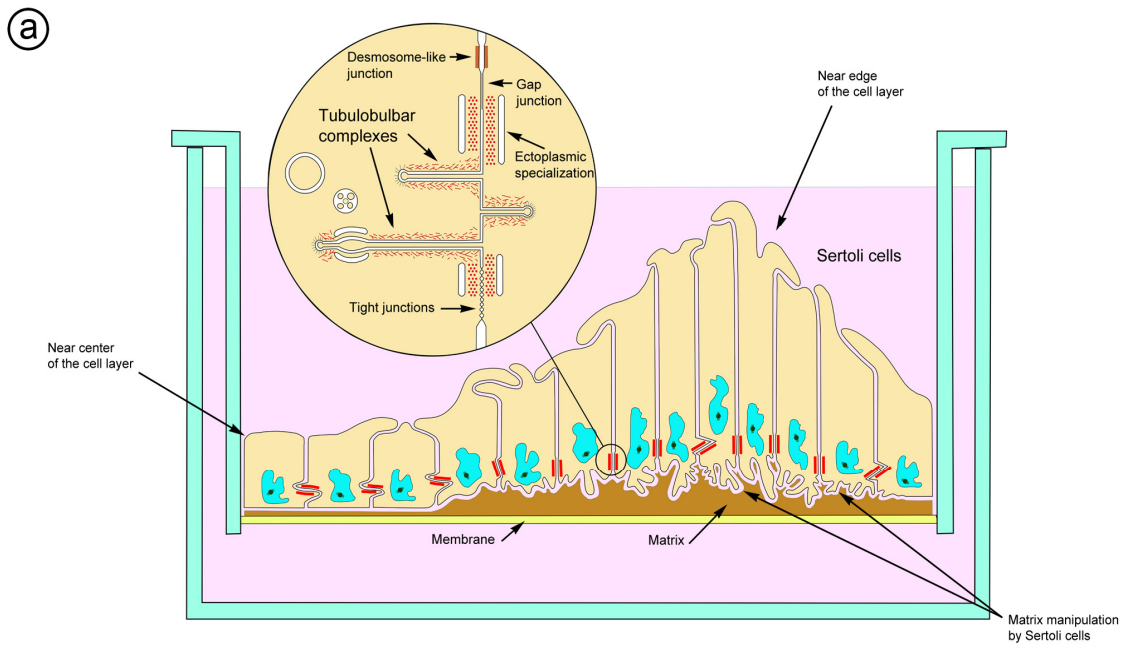


FIG. 7. Primary cultures of Sertoli cells grown on Matrigel<sup>TM</sup> in transwells are morphologically differentiated and form basal junction complexes. (a) Shown here is a schematic diagram showing the positions of junctions and tubulobulbar complexes in primary cultures of Sertoli cells. As depicted by the schematic diagram in (a) and by the images of plastic sections in (b,c,d), the heights of the cells vary in different regions of the monolayer. Low columnar cells are often present near the center of the cell layer whereas high columnar cells are often present near the periphery of the cell layer. Sertoli cells appear to manipulate Matrigel<sup>TM</sup> by extending processes into the underlying Matrigel<sup>TM</sup> layer. Bar = 20  $\mu$ m. (e) Intercellular junction complexes, recognized by the presence of ectoplasmic specializations (arrowheads), occur near the base of the monolayer. Bar = 1  $\mu$ m. Bar in inset = 100 nm. (f,g) Morphologically identifiable tight junctions (arrowheads) occur within the junction complexes. Bars = 100 nm.

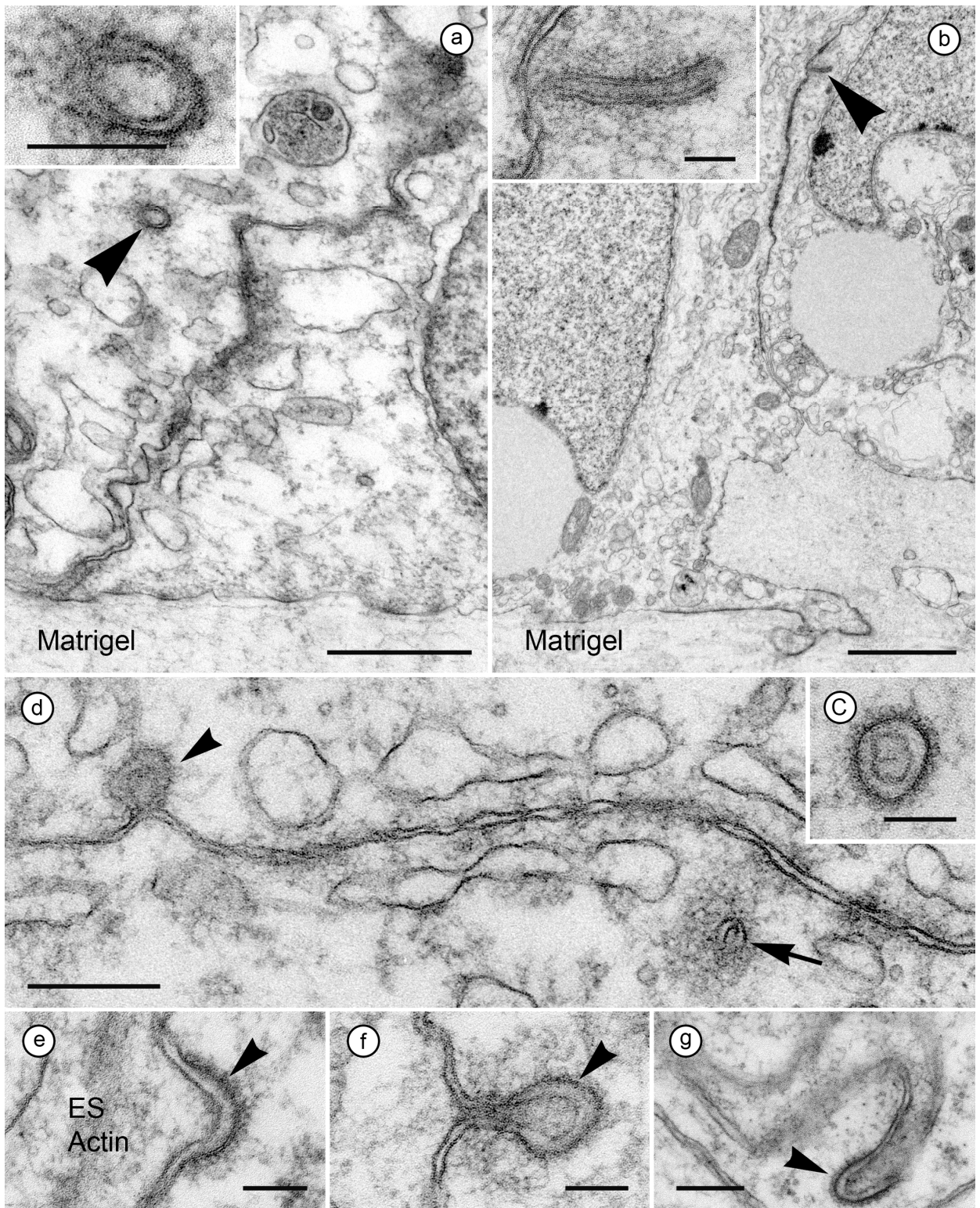


FIG. 8. Ultrastructural evidence for the formation of tubulobulbar complexes at intercellular junctions in primary cultures of Sertoli cells. (a,b) Shown here are two examples of tubulobulbar complexes (arrowheads and insets) near the bases of cultured Sertoli cells. In both cases the

sections are of the proximal tubular region and can be identified by the surrounding network of actin filaments and the double plasma membrane cores. (a) Bar = 0.5  $\mu$ m. Bar in inset = 100 nm. (b) Bar = 2  $\mu$ m. Bar in inset = 100 nm. (c) Cross section through the coated pit region of a tubulobulbar complex. Bar = 100 nm. (d) Two tubulobulbar complexes shown at a junction complex. The one indicated by the arrowhead is in the initial stages of formation whereas the one indicated by the arrow is somewhat further developed. Bar = 250 nm. (e) A tubulobulbar complex in the initial stages of formation adjacent to an actin bundle of an ectoplasmic specialization in the adjacent cell. The two cells remain connected in the region of the coated pit. Bar = 100 nm. (f) A tubulobulbar complex at a later stage than that shown in (e). Here the short tubular region has developed an actin cuff as the coated pit moves away from the junction. Bar = 100 nm. (g) In this image, the coated pit region of a tubulobulbar complex has moved away from the junction and developed a long tubular region. Bar = 200 nm.

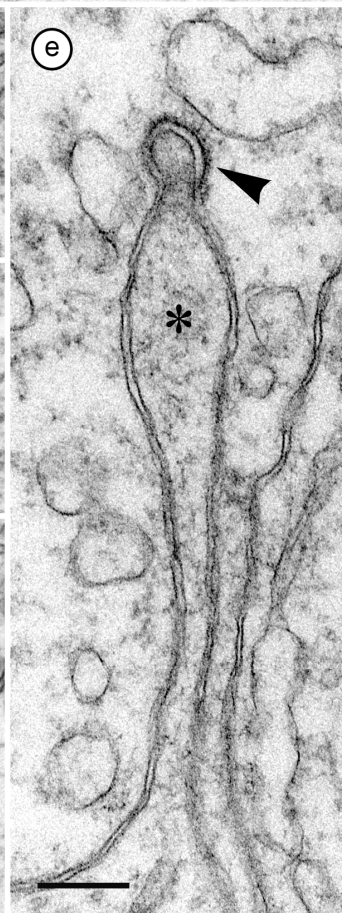
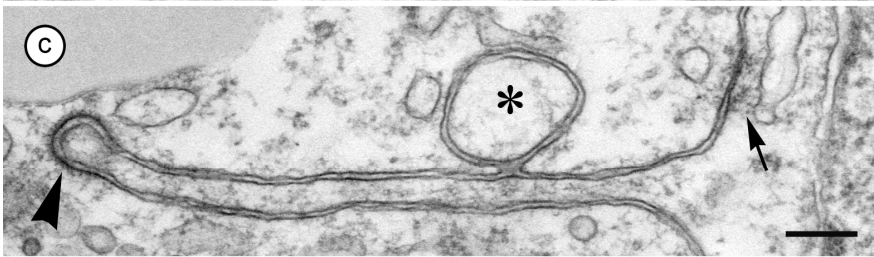
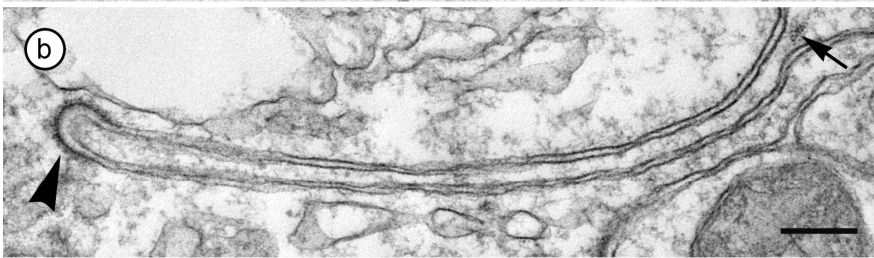
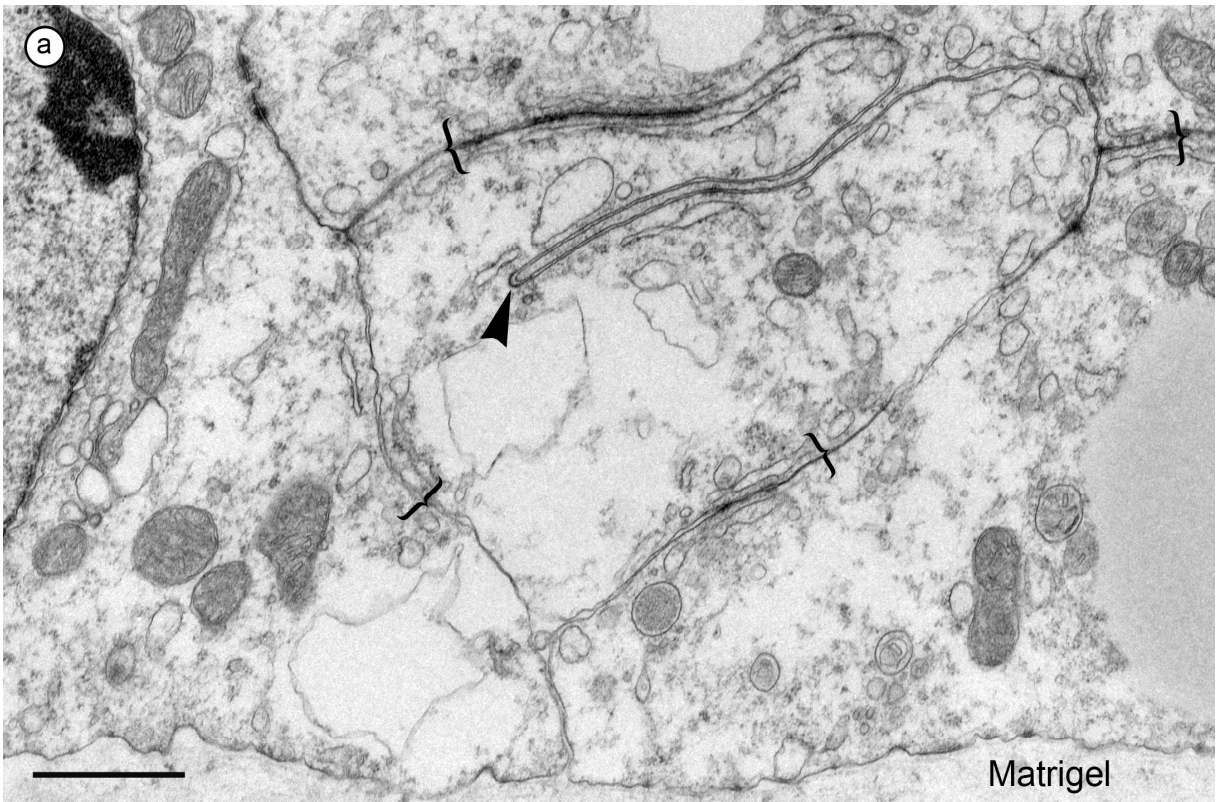


FIG. 9. Electron microscopic images of tubulobulbar-like structures in primary cultures of Sertoli cells. (a) A tubulobulbar-like structure that ends in a coated pit occurs in a pocket or fold in an intercellular junction complex (indicated by the brackets). This is similar to the location of tubulobulbar complexes observed *in vivo*. Bar = 1 mm. (b,c,d,e) Four examples of tubulobulbar-like structures in cultured Sertoli cells. The structures end in coated pits (arrowheads), are composed of double plasma membrane cores, and formed in areas where ectoplasmic specializations (arrows indicate actin bundles) are present. An ectopic bulb (asterisk) is present on the structure in (c) and a putative bulb (asterisk) is present in (e). Bars in (b,c,d) = 200 nm. Bar in (e) = 250 nm.



FIG. 10. Electron micrographs of tubulobulbar complexes in primary cultures of Sertoli cells showing the presence of ‘membrane kisses’ (arrowheads) indicative of tight junctions and similar to those observed at similar locations *in vivo*. (a) Longitudinal section through a tubulobulbar complex. Bar = 500 nm. (b,c) Cross-sections through tubulobulbar complexes. Bars = 100 nm.

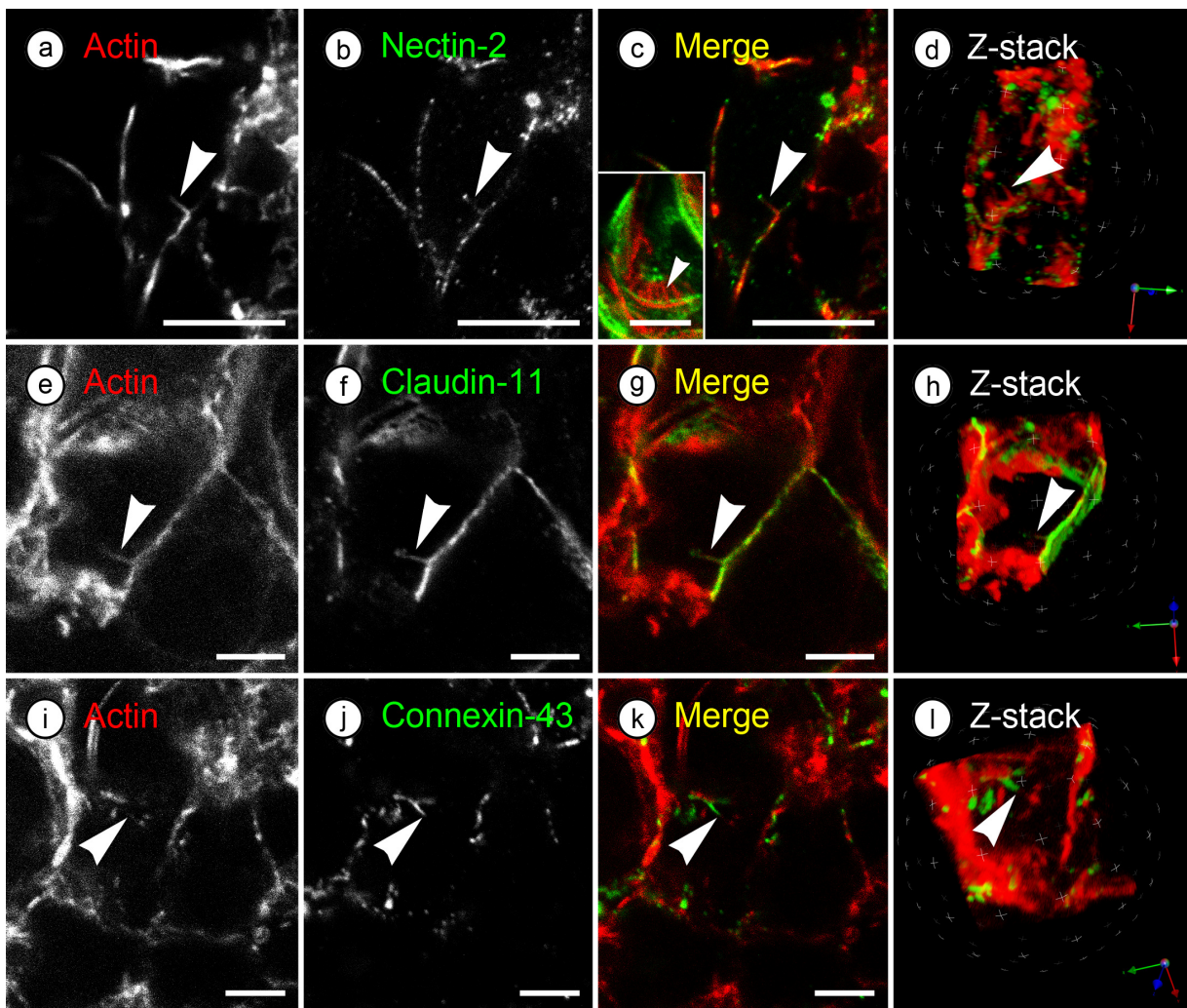


FIG. 11. Confocal (single plane) images of putative tubulobulbar complexes between cultured Sertoli cells. Single-channel images (a,b) and the resulting merged image (c) showing a rod-like protrusion extending away from the cell periphery. The rod-like protrusion is positive for filamentous actin as well as nectin-2, and resembles apical tubulobulbar complexes that are probed for the same junction elements (arrowhead in inset). Bars = 10  $\mu\text{m}$ . Bar in inset in (c) = 5  $\mu\text{m}$ . Single-channel images (e,f) and the resulting merged image (g) showing a rod-like protrusion extending away from the cell periphery. The rod-like protrusion is positive for filamentous actin as well as claudin-11. Bars = 5  $\mu\text{m}$ . Single-channel images (i,j) and the resulting merged image (k) showing a rod-like protrusion extending away from the cell periphery. The rod-like protrusion is positive for filamentous actin as well as connexin-43. Bars

= 5  $\mu$ m. (d,h,l) Single ‘snap-shot’ images of three-dimensional reconstructions of Z stacks from which the single planes in panels c,g,and k were obtained. The three dimensional reconstructions were rotated to different viewing angles to show that the protrusion is in fact rod-like and not part of a junction band. White spherical grids and XYZ axes are included in the figures to show that these images are from three-dimensional constructions.

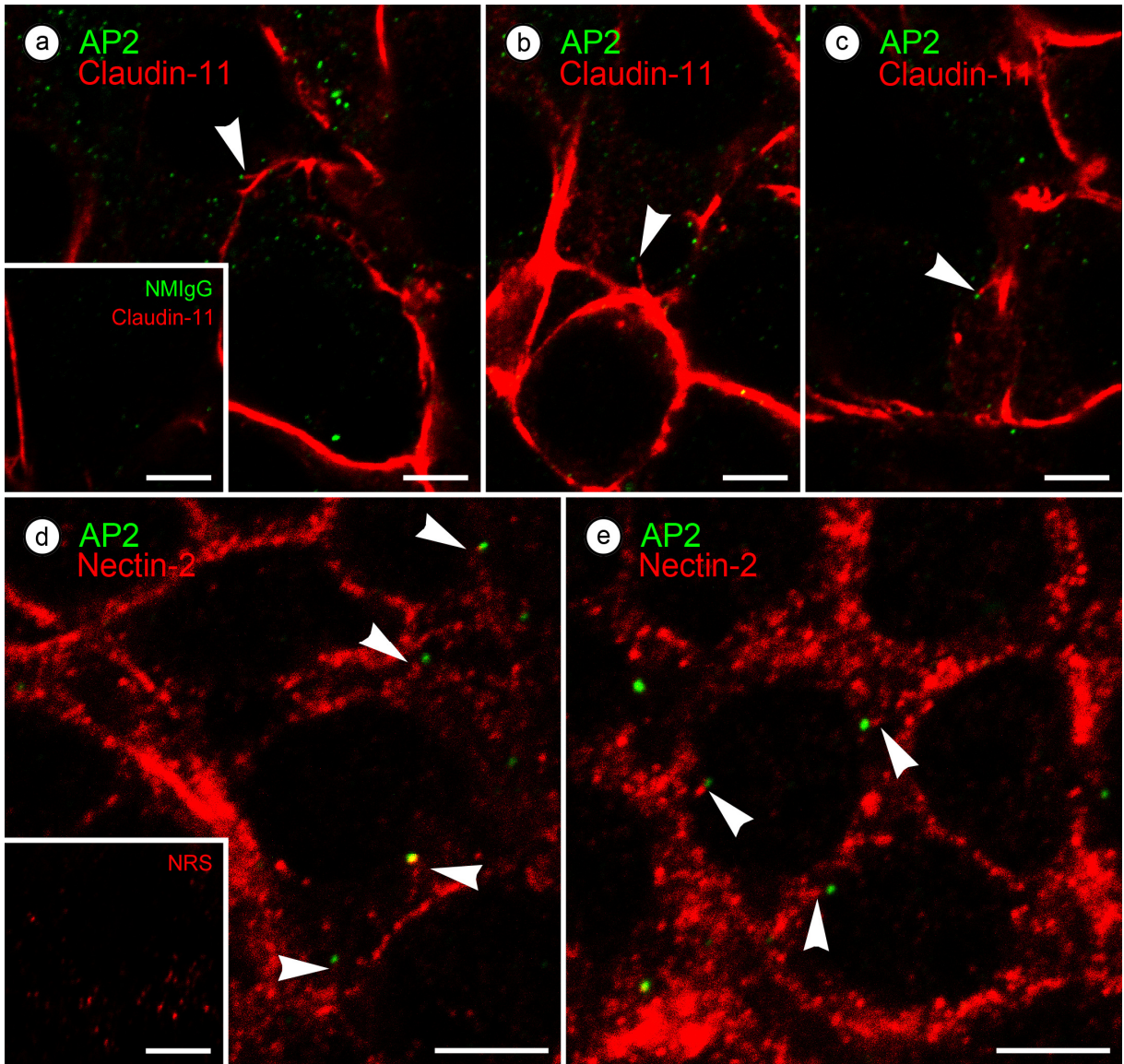


FIG. 12. Confocal images of cultured Sertoli cells labeled for AP2 and either claudin-11 (a,b,c) or nectin-2 (d,e). Arrowheads indicate rod-like structures labeled for junction proteins that also

react at their tips with the probe to AP2. Insets in (a,d) show normal IgG or serum controls in cultured Sertoli cells. Normal mouse IgG (NMIgG) and normal rabbit serum (NRS) were used to control for the staining of AP2 and nectin-2, respectively. Bars = 5  $\mu$ m.

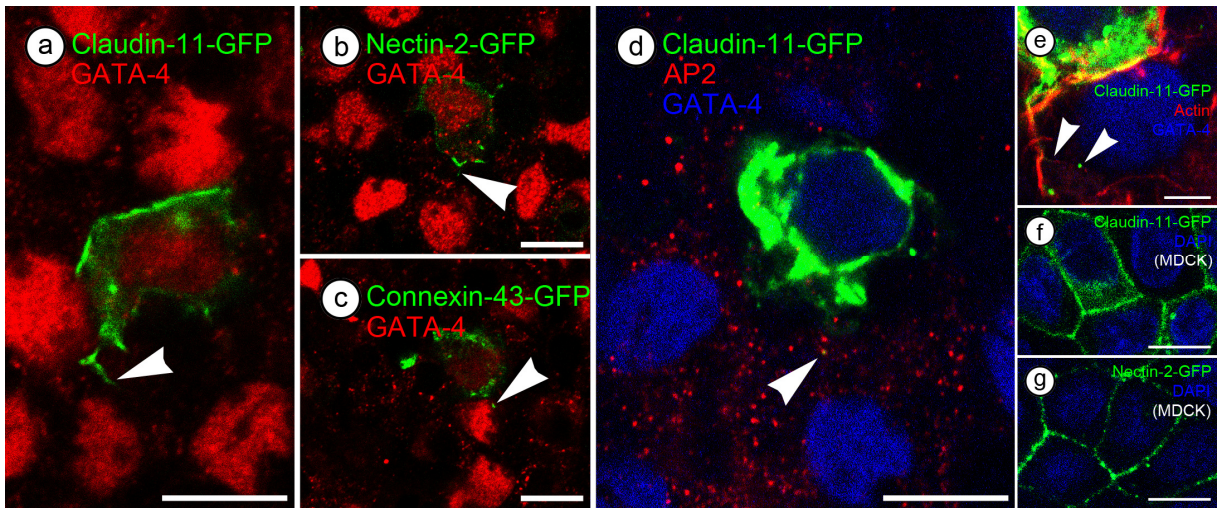


FIG. 13. Confocal images showing cultured Sertoli cells transfected with DNA plasmids encoding GFP-tagged junction proteins extend rod-like structures into adjacent non-transfected Sertoli cells. Bars = 10  $\mu$ m in (a-d and f-g). Bar = 5  $\mu$ m in (e). GATA-4 was used as a somatic cell marker and labels Sertoli cell nuclei. AP2 was used as a tubulobulbar complex marker and localizes to the ends of tubulobulbar complexes. (a,b) GFP-tagged claudin-11 (a) or nectin-2 (b) proteins are prominent at the periphery of the transfected Sertoli cells and extend rod-like protrusions (arrowheads) into adjacent non-transfected Sertoli cells. (c) GFP-tagged connexin-43 proteins are prominent at the periphery of a transfected Sertoli cell and a GFP-positive vesicle (arrowhead) was observed within an adjacent non-transfected Sertoli cell. (d,e) GFP-tagged claudin-11 proteins are prominent at the periphery of the transfected Sertoli cells and GFP-positive vesicles are present in adjacent non-transfected Sertoli cells (arrowheads). The GFP-positive vesicles associate with AP2 (arrowhead in d) or a rod-like protrusion positive for

filamentous actin (arrowheads in e). (f,g) Cultured MDCK cells were transfected with the same GFP-tagged claudin-11 (f) or GFP-tagged nectin-2 (g) fusion constructs that were used to transfect cultured Sertoli cells. Transfection with the fusion constructs were successful and GFP-tagged junction proteins localized to the MDCK cell periphery as expected.

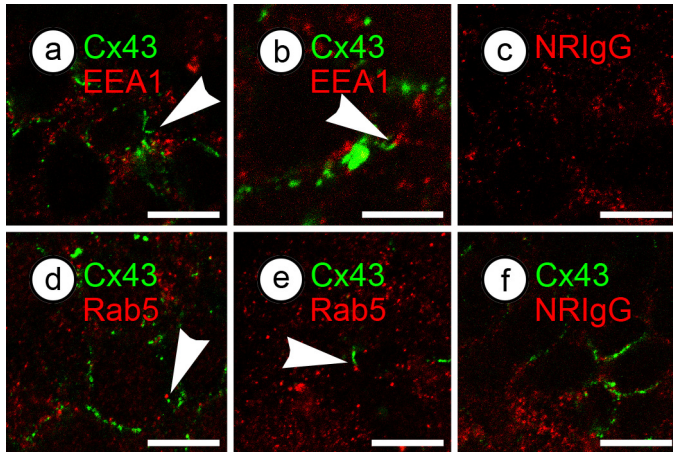


FIG. 14. Confocal images of cultured Sertoli cells showing possible tubulobulbar complexes capped at their ends by the endocytic markers EEA1 or Rab5. Bars = 10  $\mu\text{m}$  in a and c-f. Bar = 5  $\mu\text{m}$  in b. (a,b,d,e) Immunofluorescent signals of EEA1 (a,b) or Rab5 (d,e) appear

to cap the ends of rod-like protrusions positive for connexin-43 (Cx43) that extend away from the cell periphery. (c,f) Normal rabbit IgG (NRIgG) controls for the staining of EEA1 (c) and Rab5 (f) in cultured Sertoli cells. The ‘spotty’ appearance of NRIgG signals make it difficult to conclude with certainty that the signals observed in a, b, d and e specifically identify EEA1 or Rab5.

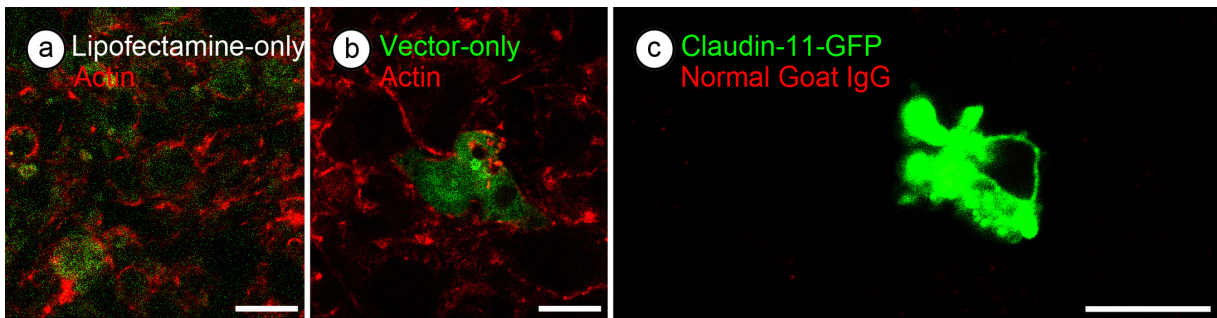


FIG. 15. Confocal images of cultured Sertoli cells showing controls for *in vitro* transfection applications. Bars = 10  $\mu$ m. (a) Cultured Sertoli cells treated with Lipofectamine<sup>TM</sup> 2000 without DNA plasmids. During image acquisition, ‘gain’ and ‘offset’ levels were erroneously increased and a diffuse pattern of background fluorescence can be seen over all cells. (b) Cultured Sertoli cells treated with empty DNA vectors that do not contain a fusion construct of interest. Empty vectors do encode EGFP. (c) Normal goat IgG (NGIgG) control in cultured Sertoli cells that were transfected with the GFP-tagged claudin-11 fusion construct. NIGgG was used to control for the staining of GATA-4 (Fig. 13, a-e).

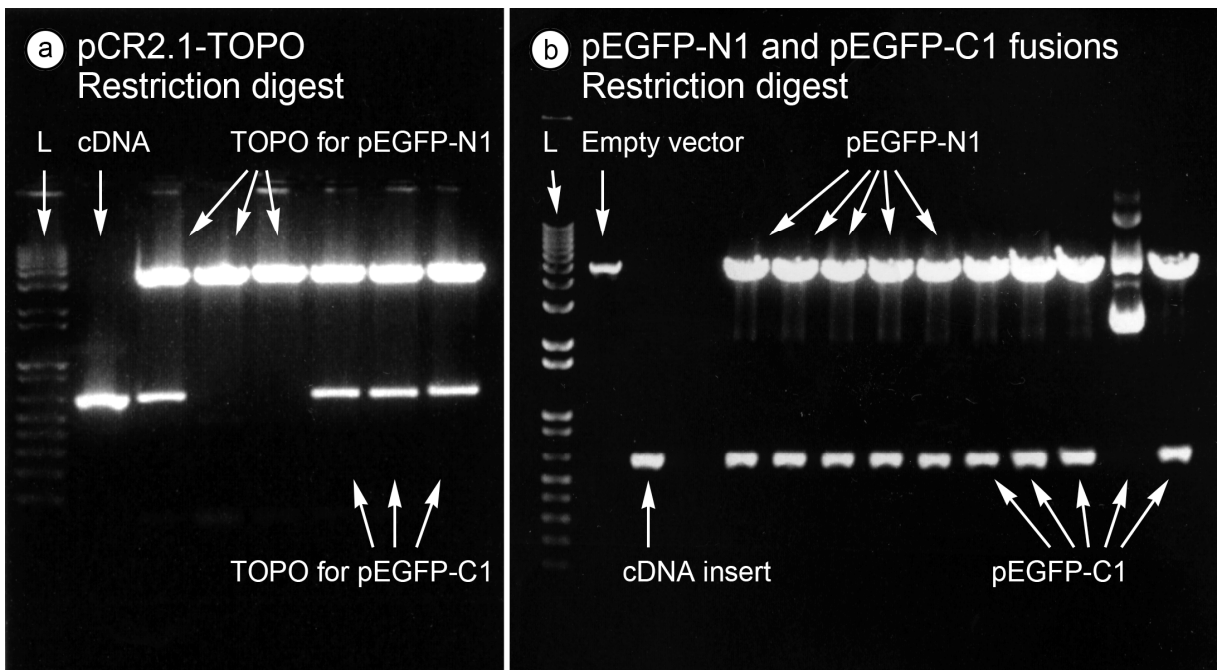


FIG. 16. Restriction digests of the pCR2.1-TOPO, pEGFP-N1 and pEGFP-C1 vectors used in the making of the claudin-11-GFP fusion construct. This is to verify the successful insertion of the claudin-11 cDNA into these vectors. 'L' = ladder. (a) Restriction digest of pCR2.1-TOPO vectors after the ligation reaction with PCR-amplified claudin-11 cDNA. 'TOPO for pEGFP-N1' and 'TOPO for pEGFP-C1' refer to the pCR2.1-TOPO vectors that would be used to sub-clone the claudin-11 cDNA into pEGFP-N1 or pEGFP-C1 vectors, respectively. Each type of TOPO vector was extracted from three independent bacterial colonies for testing. PCR-amplified claudin-11 cDNA (cDNA) was used as a control for the inserts that should be present within the vectors. One cDNA-positive sample from each types of TOPO vectors was selected for the subsequent sub-cloning process. (b) Restriction digest of pEGFP-N1 and pEGFP-C1 vectors after the sub-cloning process. A pEGFP vector that does not contain a DNA insert (Empty vector) and claudin-11 cDNA (cDNA insert) were used as references for parts of the sub-cloned vectors. Each type of the sub-cloned pEGFP vectors was extracted from five independent bacterial colonies for testing. One cDNA insert-positive sample from of each type of pEGFP vectors was selected for use in the subsequent transfection experiments.

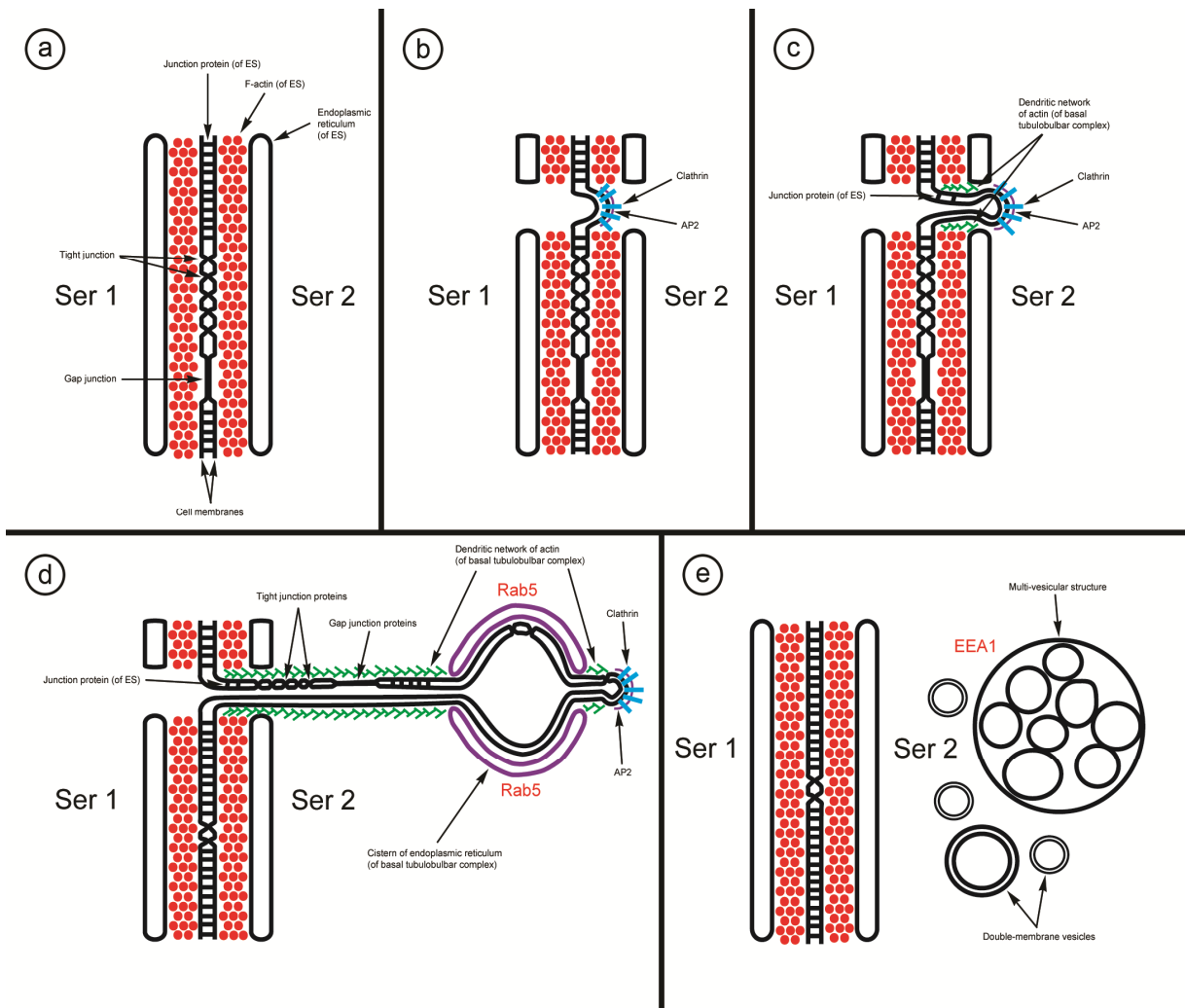


FIG. 17. Schematic representation of major steps during basal tubulobulbar complex-mediated junction internalization. ‘Ser 1’ represents one Sertoli cell. ‘Ser 2’ represents another Sertoli cell that is immediately adjacent to and forms a basal junction complex with ‘Ser 1.’ (a) Appearance of a basal junction complex prior to internalization. Major components of the basal junction complex include tight junction, gap junction and ectoplasmic specialization (ES). (b) A double-membrane clathrin-coated pit forms in the region occupied by the basal junction complex. The location of AP2 is also shown. (c) The double-membrane clathrin-coated pit invaginates into one of the attached Sertoli cells and a short tubular ‘neck’ begins to form. Junction proteins of the ectoplasmic specialization (such as nectin-2) may enter this ‘neck.’ A dendritic network of filamentous actin that surrounds the ‘neck’ also begins to form. (d) The clathrin-coated

invagination develops into a basal tubulobulbar complex complete with its proximal tubular region, bulbar region that associates with a cistern of the endoplasmic reticulum, distal tubular region and clathrin-coated tip. The entire structure has a double-membrane core. A dendritic network of actin surrounds each of the proximal and distal tubular regions. Morphologically identifiable tight and gap junctions as well as junction proteins of the ectoplasmic specialization are being internalized by this basal tubulobulbar complex. Rab5 is suspected to localize to the bulbar region of the basal tubulobulbar complex. (e) The bulbar region of the basal tubulobulbar complex buds off to form a vesicle, which may coalesce with vesicles from other basal tubulobulbar complexes to form a multi-vesicular structure. The rest of the basal tubulobulbar complex also vesiculates, resulting in the formation of numerous double-membrane vesicles. EEA1 is suspected to localize to these vesicles or vesicular structures.

## CHAPTER 6: CONCLUDING CHAPTER

Research efforts on tubulobulbar complexes have largely focused on those present at the the spermatid-Sertoli cell interface at the apical surface of the seminiferous epithelium. Some considered the complexes to be anchoring devices [28, 71, 72] or devices that reduce spermatid cytoplasm or acrosomal material [27, 73, 74], different from my view of the structures as junction internalization machinery. Studies from our own research group as well as international groups have revealed increasing amounts of information regarding the characteristics of apical tubulobulbar complexes [31, 34, 60, 67, 75-77] and of evidence to support the hypothesis that tubulobulbar complexes play a role in the junction internalization events that occur in the seminiferous epithelium [31, 32, 36]. Work presented here contribute to these efforts by consolidating our knowledge of basal tubulobulbar complexes to support the junction internalization hypothesis.

### **Relevance and contributions to the field**

Contrary to the attention received by apical tubulobulbar complexes, basal tubulobulbar complexes have been much less studied due to the reasons described in the Introduction. In addition, unlike apical tubulobulbar complexes that only occur in relationship to adhesion junctions, basal tubulobulbar complexes occur in association with junction complexes that consist of tight, gap and adhesion junctions. Up to now, there has been no *in vitro* model system(s) with which to study basal tubulobulbar complexes. It is therefore of considerable significance that this work demonstrates the feasibility of using a primary rat Sertoli cell culture system for the study of basal tubulobulbar complexes to colleagues in our research field. This *in vitro* system offers numerous advantages and future prospects to existing *in vivo* techniques.

Examples of such advantages include an easier way to identify putative basal tubulobulbar complexes from intercellular junctions, improved three-dimensional reconstruction to better visualize tubulobulbar complexes within the context of an entire Sertoli cell, an option to test the potential influence of various cell types (such as peritubular cells and germ cells) on the development and function of tubulobulbar complexes by controlling cell type composition of the cultures, ability to perform transient DNA transfection experiments, a possibility for live cell imaging to observe tubulobulbar complex development in real-time, ease of cell manipulation biochemically by altering the components of the cell culture media, and more. In addition, the conclusion that basal tubulobulbar complexes internalize intercellular junctions into one or the other of the attached Sertoli cells strengthen my support for the junction internalization hypothesis, adding evidence from a different aspect of the seminiferous epithelium than the apical aspect that most are familiar with. This brings us closer to finally ending the controversy regarding the true function of tubulobulbar complexes. This work would also bring basal tubulobulbar complexes back into the interest of colleagues in the field, whom have largely neglected the structures in the past forty years. Furthermore, the observation that the significant reduction in junctional material from Stage V to Stage VII in the seminiferous epithelium correlates temporally with the sharp rise in basal tubulobulbar complex count in Stages IV-V (first reported by Russel [29]) leads me to rethink the currently accepted model for spermatocyte translocation. I suspect that the spermatocyte translocation event is a multi-step process, with significant amounts of junction removal, likely achieved through basal tubulobulbar complexes, occurring well before the actual translocation. This improves upon the the classic idea that the event simply involves the disassembly of Sertoli-Sertoli cell junctions above the translocating spermatocyte and the reassembly of junctions below [25].

## **Overview of results and conclusions**

Conclusions derived from this study successfully fulfilled the goals stated in the Introduction. I showed that it is indeed possible to study basal tubulobulbar complexes by using a cell culture model, which others can use and improve upon in the future to further elucidate characteristics of tubulobulbar complexes. Although imperfectly, the basal tubulobulbar complexes *in vitro* do resemble their *in vivo* counterparts with respect to several defining features and are justified in their worth as a tool in research. I used a plethora of techniques on both *in vivo* and *in vitro* samples to obtain strong evidence in support of the junction internalization hypothesis that I set out to test and showed that basal tubulobulbar complexes contain junction proteins. Specifically, clear ultrastructural visualizations of intercellular junctions and basal tubulobulbar complexes achieved with electron microscopy, fluorescence data that utilized different immunofluorescent probes and markers as well as DNA transfection results employing the use of GFP-tagged junction protein fusion constructs allowed me to reach my conclusion that basal tubulobulbar complexes play a role in internalization of basal junctions in the seminiferous epithelium. I showed that, as expected, endocytic elements associate with basal tubulobulbar complexes and that junction proteins from one Sertoli cell are internalized into another Sertoli cell by these complexes. The statistical comparison of the amounts of junctional material present at Stages V and VII in the seminiferous epithelium further solidifies my conclusion.

## **Limitations**

One challenge encountered during this thesis work was the difficulty of transfecting primary cultures of rat Sertoli cells. Not only was the transfection efficiency extremely low, any one transfected Sertoli cell must also be forming at least one tubulobulbar complex with an

adjacent Sertoli cell at the time of fixation in order to provide useful information. This led to a very slow rate at which some sort of meaningful data could be harvested from DNA transfection experiments *in vitro*. Moreover, the remaining germ cells and sometimes even myoid cells that were present in culture would be transfected with higher efficiencies than Sertoli cells, resulting in sources of visual contamination when examining the samples under a microscope. Another obstacle arose when *in vitro* samples were immunoprobed for proteins and the resulted staining pattern does not differ significantly from that of normal IgG controls, such as the endocytic markers EEA1 and Rab5 (Fig. 14). This led to a situation where I could not confidently distinguish between true experimental fluorescent signals and non-specific signals. A possible cause of this obstacle may be the inability of *in vitro* tubulobulbar complexes to fully develop their bulbar regions in this current culture system. Another drawback of the *in vitro* component of this study is the imperfect removal of contaminating cells (germ cells and myoid cells) from cultures. However, the remaining contaminating cells may actually play a small, perhaps trivial role in stimulating tubulobulbar complex formation by remotely resembling cellular composition in intact seminiferous epithelia, after the native amounts of these cells as would be *in vivo* were drastically reduced. Despite these limitations, the electron microscopic data, immunofluorescence images and statistical analysis that I did present based on *in vivo* as well as *in vitro* studies are more than sufficient to support my conclusions.

### **Future directions**

Results from this study could lead to more vigorous future efforts to study basal tubulobulbar complexes. RNAi knock-down experiments targeting tubulobulbar complex components (such as cortactin [36]) could be used to examine effects of a temporary loss of basal tubulobulbar complexes on spermatocyte translocation in live animals. In these experiments I

would expect to see reduced basal tubulobulbar complex lengths at the blood-testis barrier in seminiferous epithelia, similar to what was observed in apical complexes [36]. Data could be acquired with electron microscopy, or with immunofluorescence techniques when using AP2 as a marker for tubulobulbar complexes. Statistical analysis could be performed to measure the significance of such possible size reductions. *In vitro* experiments also could be used to verify that the knock-down does affect basal tubulobulbar complex length. It is also possible that the knock-down would reduce or even eliminate the peak in appearance of basal tubulobulbar complexes in Stages IV-V that was observed by Russell [29]. Based on my conclusion that basal tubulobulbar complexes internalize components of basal junction complexes in the seminiferous epithelia, I would also expect to see a delay in spermatocyte translocation across the blood-testis barrier in live animals and perhaps an accumulation of early primary spermatocytes in basal compartments of the epithelia over time. It may be necessary to prolong the administration of RNAi reagents in order to observe an effect. Furthermore, live cell imaging experiments where real-time visualizations of the uptake of junctional material by basal tubulobulbar complexes could be achieved with the *in vitro* system.

Within intact and functional intercellular junctions, junction proteins often associate with various adaptor proteins, such as ZO-1 and afadin. It would be interesting to reveal potential relationships between these adaptor proteins and basal tubulobulbar complexes, and to examine whether basal tubulobulbar complexes internalize components of basal junctions other than integral membrane junction proteins. Adaptor proteins could be detected with immunological probes while using filamentous actin or AP2 as markers for basal tubulobulbar complexes. It would also be possible to transfect cultured Sertoli cells with DNA plasmids that encode fluorescent protein-tagged adaptor proteins, and determine whether the fluorescent protein fusion

constructs enter non-transfected cells, which would be an observation that supports the junction internalization hypothesis.

Double-transfection experiments could be performed where, for example, a GFP-tagged junction protein fusion construct and an RFP-tagged AP2 fusion construct could be simultaneously transfected into cultured Sertoli cells. In successfully double-transfected Sertoli cells that are visualized in real-time, GFP signals representing junction proteins should localize to the cell periphery, and may be observed to gradually extend away from the cell periphery into rod-like protrusions capped at their ends by RFP signals representing AP2. Moreover, instead of transfecting cells that grow on Matrigel<sup>TM</sup> in bicameral chambers, it would be possible to transfect cells that are suspended in culture media. For example, one cell population could be transfected with a GFP-tagged junction protein fusion construct, while another cell population with a RFP-tagged junction protein fusion construct (or entirely untransfected). The two cell populations in suspension could be mixed together and cultured in the same chamber. If one type of fusion construct is present in cells that either produce the other type of fusion construct or are otherwise untransfected, then such data would support the junction internalization hypothesis. Of course, the major difficulty associated with this approach would be the extremely low transfection rates in primary cultures of rat Sertoli cells. To help resolve this difficulty, it may be necessary to seek out alternative means of DNA transfection such as the magnetism-based transfection equipment offered by PromoCell GmbH (Sickingenstraße, Heidelberg, Germany). It may also be possible to use live cell imaging techniques to track GFP-tagged junction proteins after they have been internalized by tubulobulbar complexes to see if they are degraded by lysosomes (loss of GFP signals) or if they are stored (GFP signals remain in cytoplasm) and eventually re-inserted into the cell membrane (GFP signals re-enter cell periphery). This would

help us to better understand if junction elements internalized by tubulobulbar complexes enter the degradation pathway or recycling pathway.

Moreover, future efforts could be aimed at attempting to recreate, at least to some degree, the complex Sertoli-germ cell organization of intact seminiferous epithelia. Spermatogonial cells could be seeded first onto Matrigel<sup>TM</sup>, followed by Sertoli cells on top. Experimental adjustments made to this setup could allow the simulation of a seminiferous epithelial basal compartment that contains spermatogonia *in vitro*. Subsequently, spermatogonia may develop into spermatocytes and eventually into spermatozoa that are released into the culture media. This would allow us to analyze if germ cells have any influence on the development of basal tubulobulbar complexes and in particular, whether the presence of germ cells could lead to the formation of a bulbar region which is not often seen on tubulobulbar complexes in the current *in vitro* system. Similar cell type composition adjustments could be applied to myoid cells as well. In addition, *in vivo* and *in vitro* samples could be probed for suspected components of or proteins that associate with both apical and basal tubulobulbar complexes to study whether they share all components or if one contains exclusive components that are not present in the other.

### **A potential contraceptive target**

Being what I think of as essential participants in spermatogenesis, basal tubulobulbar complexes are also located closer to the blood stream than their apical counterparts. This may have significant implications for basal complexes as potential targets for contraception. If future orally ingested contraceptive medicine are designed to target basal tubulobulbar complexes, medicinal substances carried by the blood stream may reach basal complexes faster than they would apical complexes, therefore initiating a quicker onset of drug activities that can be

controlled more accurately. Contraceptives that act on basal tubulobulbar complexes could potentially exert their effects by reversibly hinder the formation and development of the structures, resulting in delayed junction turnover of the basal junction complexes in the seminiferous epithelia. This would lead to a temporary cease in spermatocyte translocation across the blood-testis barrier and subsequently a reduction in sperm count over a limited period of time. This could be very useful for future-dated conception prevention. It may not be unlikely that the same contraceptives would also target apical tubulobulbar complexes, which have been shown to result in failed spermiation when a component is knocked-down [36], resulting in lowered sperm count and thus further enhancing the effectiveness of the drugs.

## REFERENCES

1. Ivanov AI, Nusrat A, Parkos CA. Endocytosis of epithelial apical junctional proteins by a clathrin-mediated pathway into a unique storage compartment. *Mol Biol Cell* 2004; 15:176-188.
2. Le TL, Yap AS, Stow JL. Recycling of E-cadherin: a potential mechanism for regulating cadherin dynamics. *J Cell Biol* 1999; 146:219-232.
3. Marchiando AM, Shen L, Graham WV, Weber CR, Schwarz BT, Austin JR, 2nd, Raleigh DR, Guan Y, Watson AJ, Montrose MH, Turner JR. Caveolin-1-dependent occludin endocytosis is required for TNF-induced tight junction regulation in vivo. *J Cell Biol* 2010; 189:111-126.
4. Shen L, Turner JR. Actin depolymerization disrupts tight junctions via caveolae-mediated endocytosis. *Mol Biol Cell* 2005; 16:3919-3936.
5. Bruewer M, Utech M, Ivanov AI, Hopkins AM, Parkos CA, Nusrat A. Interferon-gamma induces internalization of epithelial tight junction proteins via a macropinocytosis-like process. *Faseb J* 2005; 19:923-933.
6. Paterson AD, Parton RG, Ferguson C, Stow JL, Yap AS. Characterization of E-cadherin endocytosis in isolated MCF-7 and chinese hamster ovary cells: the initial fate of unbound E-cadherin. *J Biol Chem* 2003; 278:21050-21057.
7. Utech M, Ivanov AI, Samarin SN, Bruewer M, Turner JR, Mrsny RJ, Parkos CA, Nusrat A. Mechanism of IFN-gamma-induced endocytosis of tight junction proteins: myosin II-dependent vacuolarization of the apical plasma membrane. *Mol Biol Cell* 2005; 16:5040-5052.
8. Berthoud VM, Minogue PJ, Laing JG, Beyer EC. Pathways for degradation of connexins and gap junctions. *Cardiovasc Res* 2004; 62:256-267.

9. Gaietta G, Deerinck TJ, Adams SR, Bouwer J, Tour O, Laird DW, Sosinsky GE, Tsien RY, Ellisman MH. Multicolor and electron microscopic imaging of connexin trafficking. *Science* 2002; 296:503-507.
10. Larsen WJ, Tung HN, Murray SA, Swenson CA. Evidence for the participation of actin microfilaments and bristle coats in the internalization of gap junction membrane. *J Cell Biol* 1979; 83:576-587.
11. Piehl M, Lehmann C, Gumpert A, Denizot JP, Segretain D, Falk MM. Internalization of Large Double-Membrane Intercellular Vesicles by a Clathrin-dependent Endocytic Process. *Mol Biol Cell* 2007; 18:337-347.
12. Vogl AW, Pfeiffer DC, Redenbach DM. Ectoplasmic ("junctional") specializations in mammalian Sertoli cells: influence on spermatogenic cells. *Ann N Y Acad Sci* 1991; 637:175-202.
13. Dym M, Fawcett DW. The blood-testis barrier in the rat and the physiological compartmentation of the seminiferous epithelium. *Biol Reprod* 1970; 3:308-326.
14. Cheng CY, Mruk DD. Cell junction dynamics in the testis: Sertoli-germ cell interactions and male contraceptive development. *Physiol Rev* 2002; 82:825-874.
15. Vogl AW, Vaid KS, Guttman JA. The Sertoli cell cytoskeleton. In: Cheng CY (ed.) *Molecular mechanisms in spermatogenesis*, vol. 636. Austin, Texas: Landes Bioscience; 2008: 186-211.
16. Morita K, Sasaki H, Fujimoto K, Furuse M, Tsukita S. Claudin-11/OSP-based tight junctions of myelin sheaths in brain and Sertoli cells in testis. *J Cell Biol* 1999; 145:579-588.
17. Ozaki-Kuroda K, Nakanishi H, Ohta H, Tanaka H, Kurihara H, Mueller S, Irie K, Ikeda W, Sakai T, Wimmer E, Nishimune Y, Takai Y. Nectin couples cell-cell adhesion and the actin scaffold at heterotypic testicular junctions. *Curr Biol* 2002; 12:1145-1150.

18. Kumar NM, Gilula NB. The gap junction communication channel. *Cell* 1996; 84:381-388.
19. Carette D, Weider K, Gilleron J, Giese S, Dompierre J, Bergmann M, Brehm R, Denizot JP, Segretain D, Pointis G. Major involvement of connexin 43 in seminiferous epithelial junction dynamics and male fertility. *Dev Biol* 2010; 346:54-67.
20. Pointis G, Segretain D. Role of connexin-based gap junction channels in testis. *Trends Endocrinol Metab* 2005; 16:300-306.
21. Leblond CP, Clermont Y. Definition of the stages of the cycle of the seminiferous epithelium in the rat. *Ann N Y Acad Sci* 1952; 55:548-573.
22. Clermont Y, Perey B. The stages of the cycle of the seminiferous epithelium of the rat: practical definitions in PA-Schiff-hematoxylin and hematoxylin-eosin stained sections. *Rev Can Biol* 1957; 16:451-462.
23. Clermont Y, Leblond CP, Messier B. [Duration of the cycle of the seminal epithelium of the rat]. *Arch Anat Microsc Morphol Exp* 1959; 48(Suppl):37-55.
24. Perey B, Clermont Y, Leblond CP. The wave of the seminiferous epithelium in the rat. *Am J Anat* 1961; 108:47-77.
25. Russell L. Movement of spermatocytes from the basal to the adluminal compartment of the rat testis. *Am J Anat* 1977; 148:313-328.
26. Komljenovic D, Sandhoff R, Teigler A, Heid H, Just WW, Gorgas K. Disruption of blood-testis barrier dynamics in ether-lipid-deficient mice. *Cell Tissue Res* 2009; 337:281-299.
27. Upadhyay RD, Kumar AV, Ganeshan M, Balasinor NH. Tubulobulbar complex: Cytoskeletal remodeling to release spermatozoa. *Reprod Biol Endocrinol* 2012; 10:27.
28. Russell L, Clermont Y. Anchoring device between Sertoli cells and late spermatids in rat seminiferous tubules. *Anat Rec* 1976; 185:259-278.

29. Russell LD. Observations on the inter-relationships of Sertoli cells at the level of the blood- testis barrier: evidence for formation and resorption of Sertoli-Sertoli tubulobulbar complexes during the spermatogenic cycle of the rat. *Am J Anat* 1979; 155:259-279.
30. Vogl AW, Pfeiffer DC, Redenbach DM, Grove BD. Sertoli cell cytoskeleton. In: Russell LD, Griswold MD (eds.), *The Sertoli Cell*. Clearwater FL: Cache River Press; 1993: 39 - 86.
31. Guttman JA, Takai Y, Vogl AW. Evidence that tubulobulbar complexes in the seminiferous epithelium are involved with internalization of adhesion junctions. *Biol Reprod* 2004; 71:548-559.
32. Young JS, Guttman JA, Vaid KS, Vogl AW. Tubulobulbar complexes are intercellular podosome-like structures that internalize intact intercellular junctions during epithelial remodeling events in the rat testis. *Biol Reprod* 2009; 80:162-174.
33. Young JS, Takai Y, Kojic KL, Vogl AW. Internalization of adhesion junction proteins and their association with recycling endosome marker proteins in rat seminiferous epithelium. *Reproduction* 2012; 143:347-357.
34. Kusumi N, Watanabe M, Yamada H, Li SA, Kashiwakura Y, Matsukawa T, Nagai A, Nasu Y, Kumon H, Takei K. Implication of amphiphysin 1 and dynamin 2 in tubulobulbar complex formation and spermatid release. *Cell Struct Funct* 2007; 32:101-113.
35. D'Souza R, Pathak S, Upadhyay R, Gaonkar R, D'Souza S, Sonawane S, Gill-Sharma M, Balasinor NH. Disruption of tubulobulbar complex by high intratesticular estrogens leading to failed spermiation. *Endocrinology* 2009; 150:1861-1869.
36. Young JS, de Asis M, Guttman JA, Vogl AW. Cortactin depletion results in short tubulobulbar complexes and spermiation failure in rat testis. *Biology Open* 2012; 1:1-9.

37. Dorrington JH, Roller NF, Fritz IB. Effects of follicle-stimulating hormone on cultures of Sertoli cell preparations. *Mol Cell Endocrinol* 1975; 3:57-70.
38. Steinberger A, Heindel JJ, Lindsey JN, Elkington JS, Sanborn BM, Steinberger E. Isolation and culture of FSH responsive Sertoli cells. *Endocr Res Commun* 1975; 2:261-272.
39. Djakiew D, Hadley MA, Byers SW, Dym M. Transferrin-mediated transcellular transport of <sup>59</sup>Fe across confluent epithelial sheets of Sertoli cells grown in bicameral cell culture chambers. *J Androl* 1986; 7:355-366.
40. Galdieri M, Ziparo E, Palombi F, Russo MA, Stefanini M. Pure Sertoli-Cell Cultures - a New Model for the Study of Somatic-Germ Cell-Interactions. *Journal of Andrology* 1981; 2:249-254.
41. Chung SS, Lee WM, Cheng CY. Study on the formation of specialized inter-Sertoli cell junctions in vitro. *J Cell Physiol* 1999; 181:258-272.
42. Kaitu'u-Lino TJ, Sluka P, Foo CF, Stanton PG. Claudin-11 expression and localisation is regulated by androgens in rat Sertoli cells in vitro. *Reproduction* 2007; 133:1169-1179.
43. Lui WY, Lee WM, Cheng CY. Transforming growth factor beta3 regulates the dynamics of Sertoli cell tight junctions via the p38 mitogen-activated protein kinase pathway. *Biol Reprod* 2003; 68:1597-1612.
44. Sang QX, Stetler-Stevenson WG, Liotta LA, Byers SW. Identification of type IV collagenase in rat testicular cell culture: influence of peritubular-Sertoli cell interactions. *Biol Reprod* 1990; 43:956-964.
45. Skinner MK, Griswold MD. Secretion of testicular transferrin by cultured Sertoli cells is regulated by hormones and retinoids. *Biol Reprod* 1982; 27:211-221.

46. Skinner MK, Tung PS, Fritz IB. Cooperativity between Sertoli cells and testicular peritubular cells in the production and deposition of extracellular matrix components. *J Cell Biol* 1985; 100:1941-1947.
47. Izumi Y, Yamaguchi K, Ishikawa T, Ando M, Chiba K, Hashimoto H, Shiotani M, Fujisawa M. Molecular changes induced by bisphenol-A in rat Sertoli cell culture. *Syst Biol Reprod Med* 2011; 57:228-232.
48. Mruk DD, Cheng CY. An in vitro system to study Sertoli cell blood-testis barrier dynamics. *Methods Mol Biol* 2011; 763:237-252.
49. Hadley MA, Byers SW, Suarez-Quian CA, Kleinman HK, Dym M. Extracellular matrix regulates Sertoli cell differentiation, testicular cord formation, and germ cell development in vitro. *J Cell Biol* 1985; 101:1511-1522.
50. Byers SW, Hadley MA, Djakiew D, Dym M. Growth and characterization of polarized monolayers of epididymal epithelial cells and Sertoli cells in dual environment culture chambers. *J Androl* 1986; 7:59-68.
51. Janecki A, Steinberger A. Polarized Sertoli cell functions in a new two-compartment culture system. *J Androl* 1986; 7:69-71.
52. Suárez-Quian CA, Onoda M. Isolation and culture of Sertoli cells from immature rats. In: Doyle A, Griffiths JB, Newell DC (eds.), *Cell and Tissue Culture, Laboratory Procedures*. New York: John Wiley & Sons, Inc.; 1995.
53. Clermont Y, Perey B. Quantitative study of the cell population of the seminiferous tubules in immature rats. *Am J Anat* 1957; 100:241-267.
54. Nagy F. Cell division kinetics and DNA synthesis in the immature sertoli cells of the rat testis. *J Reprod Fertil* 1972; 28:389-395.

55. Gow A, Southwood CM, Li JS, Pariali M, Riordan GP, Brodie SE, Danias J, Bronstein JM, Kachar B, Lazzarini RA. CNS myelin and sertoli cell tight junction strands are absent in Osp/claudin-11 null mice. *Cell* 1999; 99:649-659.
56. Risley MS. Connexin gene expression in seminiferous tubules of the Sprague-Dawley rat. *Biol Reprod* 2000; 62:748-754.
57. Decrouy X, Gasc JM, Pointis G, Segretain D. Functional characterization of Cx43 based gap junctions during spermatogenesis. *J Cell Physiol* 2004; 200:146-154.
58. Brehm R, Ruttinger C, Kibschull M, Winterhager E, Willecke K, Guillou F, Steger K, Bergmann M. Effects of a Sertoli cell-specific knockout of the connexin43 gene on the regulation of spermatogenesis in transgenic mice using the Cre/loxP-recombination system. *Andrologia* 2005; 37:235-236.
59. Tung PS, Fritz IB. Characterization of rat testicular peritubular myoid cells in culture: alpha-smooth muscle isoactin is a specific differentiation marker. *Biol Reprod* 1990; 42:351-365.
60. Vaid KS, Guttman JA, Babyak N, Deng W, McNiven MA, Mochizuki N, Finlay BB, Vogl AW. The role of dynamin 3 in the testis. *J Cell Physiol* 2007; 210:644-654.
61. Abramoff MD, Magalhaes PJ, Ram SJ. Image processing with ImageJ. *Biophotonics International* 2004; 11:36-42.
62. Julio G, Merindano MD, Canals M, Rallo M. Image processing techniques to quantify microprojections on outer corneal epithelial cells. *J Anat* 2008; 212:879-886.
63. Particelli F, Mecozzi L, Beraudi A, Montesi M, Baruffaldi F, Viceconti M. A comparison between micro-CT and histology for the evaluation of cortical bone: effect of polymethylmethacrylate embedding on structural parameters. *J Microsc* 2012; 245:302-310.

64. Russ JC, Russ JC. Automatic discrimination of features in grey-scale images. *Journal of Microscopy* 1987; 148:263-277.
65. Pearse BM, Robinson MS. Clathrin, adaptors, and sorting. *Annu Rev Cell Biol* 1990; 6:151-171.
66. Robinson MS. Adaptable adaptors for coated vesicles. *Trends Cell Biol* 2004; 14:167-174.
67. Young JS, Guttman JA, Vaid KS, Shahinian H, Vogl AW. Cortactin (CTTN), N-WASP (WASP), and Clathrin (CLTC) Are Present at Podosome-Like Tubulobulbar Complexes in the Rat Testis. *Biol Reprod* 2009; 80:153-161.
68. Russell LD. Further observations on tubulobulbar complexes formed by late spermatids and Sertoli cells in the rat testis. *Anat Rec* 1979; 194:213-232.
69. Pelletier RM. Cyclic modulation of Sertoli cell junctional complexes in a seasonal breeder: the mink (*Mustela vison*). *Am J Anat* 1988; 183:68-102.
70. Yan HH, Mruk DD, Wong EW, Lee WM, Cheng CY. An autocrine axis in the testis that coordinates spermiation and blood-testis barrier restructuring during spermatogenesis. *Proc Natl Acad Sci U S A* 2008; 105:8950-8955.
71. Mruk DD, Cheng CY. Cell-cell interactions at the ectoplasmic specialization in the testis. *Trends Endocrinol Metab* 2004; 15:439-447.
72. Mruk DD, Cheng CY. Sertoli-Sertoli and Sertoli-germ cell interactions and their significance in germ cell movement in the seminiferous epithelium during spermatogenesis. *Endocr Rev* 2004; 25:747-806.
73. Tanii I, Yoshinaga K, Toshimori K. Morphogenesis of the acrosome during the final steps of rat spermiogenesis with special reference to tubulobulbar complexes. *Anat Rec* 1999; 256:195-201.

74. Russell LD. Spermatid-Sertoli tubulobulbar complexes as devices for elimination of cytoplasm from the head region late spermatids of the rat. *Anat Rec* 1979; 194:233-246.
75. Guttman JA, Obinata T, Shima J, Griswold M, Vogl AW. Non-muscle cofilin is a component of tubulobulbar complexes in the testis. *Biol Reprod* 2004; 70:805-812.
76. Nicholls PK, Harrison CA, Walton KL, McLachlan RI, O'Donnell L, Stanton PG. Hormonal regulation of sertoli cell micro-RNAs at spermiation. *Endocrinology* 2011; 152:1670-1683.
77. Young JS, Vogl AW. Focal adhesion proteins Zyxin and Vinculin are co-distributed at tubulobulbar complexes. *Spermatogenesis* 2012; 2:63-68.